Modelling Extreme Rainfall over Southern Africa

AM Joubert • SJ Crimp • SJ Mason

Report to the Water Research Commission
by the
Climatology Research Group
University of the Witwatersrand

WRC Report No 805/1/99

MODELLING EXTREME RAINFALL OVER SOUTHERN AFRICA

FINAL REPORT TO THE

WATER RESEARCH COMMISSION

A.M. Joubert, S.J. Crimp and S.J. Mason

Climatology Research Group,

University of the Witwatersrand

WRC Report No : 805/1/99

ISBN No : 1 86845 488 6

SUMMARY

The main objective of the Modelling Extreme Rainfall Over Southern Africa project is to improve the existing understanding of the processes responsible for the generation of heavy rainfall over southern Africa. Several heavy rainfall events over South and southern Africa have been examined, including tropical cyclone Demoina (late January 1984) and the floods of February 1996. Also included in the project was an assessment of a seasonal rainfall forecast for January-April 1996 over southern Africa produced by the United Kingdom Meteorological Office (UKMO), which failed to predict the forthcoming flood event. Lastly, an assessment of the ability of a nested regional climate model to simulate present-day daily rainfall over southern Africa is presented.

An important component of this project has been the combination of numerical modelling and kinematic trajectory analysis methods in order to improve our understanding of the source and transport of moisture associated with extreme rainfall events. The analyses presented in this report identify the subtropical western Indian Ocean as an important moisture source for heavy rainfall events. This finding is contrary to earlier research, which suggested that the tropical equatorial Indian Ocean was the primary source of moisture for (particularly late) summer rainfall over the region. Further research is required to ascertain whether the source of moisture for heavy rainfall events is event-specific, or whether the subtropical western Indian Ocean is an important moisture source for all rainfall over the subcontinent.

The assessment of the seasonal rainfall prediction issued by the UKMO identified a systematic failure in the model's control climate simulation. This would suggest that it may be inherently unable to produce reliable seasonal forecasts for the second half of the season, due to the fact that the northward progression of the westerlies during autumn occurs too early and effectively results in a premature end to the rainfall season.

Backward kinematic trajectory analysis of air mass transport associated with tropical cyclone Demoina (late January 1984) indicate that the primary source of moisture for the tropical cyclone was highly localised and associated with the vortex itself. Trajectories indicate an inflow from the east into the system from the central tropical and subtropical Indian Ocean, associated with very rapid uplift of moisture from the surface to above 500 hPa within the walls of the cyclone itself. A secondary airflow pattern from the South Atlantic region introduces colder, drier air from the south-west, which is generally descending as it reaches the location of the cyclone vortex. It is hypothesised that this inflow provides a wedge of more stable, colder air against which the uplift in the cyclone can occur.

The CSIRO limited area model (DARLAM) has been nested within the output from the CSIRO9 GCM to provide high-resolution, process-based simulations of present (and future) climate over the southern African region. In general, the regional climate model is much better-able to simulate regional climate detail than the forcing GCM, although significant problems exist in the simulation of daily rainfall totals and frequencies. DARLAM simulates too much rain, and too many rain days over much of the eastern parts of southern Africa, and the over-estimate is most severe over regions of steep orographic gradient such as the escarpment region of South Africa. While simulated circulation adjustments associated with above-average rainfall are realistic, the over-estimate in the number of rain days, and hence total daily rainfall is related to the model's inability to simulate accurately the processes associated with uplift and rainfall-production along steep orographic gradients. Further model development will be required before it can be used with confidence to provide reliable estimates of changes in daily rainfall statistics, given an enhanced greenhouse effect, over the southern Africa region.

CONTENTS

CHAPTER 1

INTRODUCTION

The Modelling Extreme Rainfall Over Southern Africa project (Water Research Commission Project Number K5/805/0/1) was launched in January 1997. The main objective of the research was to improve the existing understanding of the processes responsible for the generation of heavy rainfall over southern Africa so that forecast skill could be improved on a wide range of time scales. To achieve this objective, the Climatology Research Group (CRG) set four specific aims. These were:

1. to model the structure of extreme rainfall-producing systems over southern Africa using the Colorado State University Regional Atmospheric Modelling System (CSU RAMS);

2. to examine possible reasons for the failure of existing (current in 1996/7) models to provide accurate seasonal forecasts of very wet seasons;

3. to assess the ability of general circulation models to simulate extreme wet years on inter-annual time scales over southern Africa; and

4. to develop reliable estimates of changes in extreme rainfall under enhanced greenhouse conditions derived from general circulation model simulations.

The Project was scheduled for three years (January 1997-December 1999). Dr Simon Mason (Deputy-Director at the time of the initiation of the project) left the Group in November 1997, as did Mr Steven Crimp in May 1998. Dr Alec Joubert (currently Deputy-Director) will leave the Group in November 1998. As such, the departure of the three principal researchers involved in the Modelling Extreme Rainfall project has necessitated an application by the Group for the early closure of the project, in November 1998. As such, the results presented here, represent the final report to the

Water Research Commission on the Modelling Extreme Rainfall Over Southern Africa project.

The first two aims of the project, dealing with the use of the CSU RAMS model, and assessments of seasonal forecasts during of very wet seasons, have been met during 1997 and 1998, and results are described briefly below. In early 1997, Dr Joubert received an invitation to visit the Commonwealth Scientific and Industrial Research Organisation (CSIRO) Atmospheric Research Division in Melbourne, Australia, as a visiting scientist. During this time, he completed a number of experiments using a regional climate model nested within the CSIRO global climate model. The focus of research, therefore, has shifted away from *global* climate model of regional climate, to the simulation of regional climate using nested *regional* models. This shift is reflected in the results presented in this report. The application of a new modelling approach such as this requires a careful assessment of the performance of the model, before simulations of future regional climate by the model can be interpreted. The results presented in this report present an assessment of the ability of the model to simulate *present-day* daily-rainfall statistics, which are a key to the reliable simulation of changes in extreme events in the future.

Several important and valuable findings have been made during the project, despite the fact that it's duration has been cut by more than a third. Components of the project which have been completed can be summarised as follows:

- The CSU RAMS model has been used extensively, in conjunction with the Group's kinematic trajectory model, to improve the understanding of the moisture sources and transports associated with heavy rainfall events, such as the the flood event of 11-16 February 1996 (**Chapter 2**).

- The performance of the United Kingdom Meteorological Office (UKMO) seasonal forecasts during the February 1996 floods has been assessed, using the Group's kinematic trajectory model (**Chapter 3**).

- The kinematic trajectory model, in conjunction with NCEP reanalysis data has been used to investigate the air mass transport and moisture sources for

tropical cyclone Demoina, which produced widespread flooding over the Lowveld region of Mpumalanga, Swaziland and northern Kwazulu/Natal during late January 1984 (**Chapter 4**).

- The CSIRO Atmospheric Research Division Limited Area Model (DARLAM) has been nested within the CSIRIO 9-level global climate model (CSIRO9) to provide seasonally-varying simulations of regional climate over southern Africa under present and future climate conditions. Results presented in this report examine the simulation of daily rainfall over southern Africa, and specifically over the escarpment region of South Africa (**Chapter 5**).

CHAPTER 2

THE EXTREME PRECIPITATION EVENT OF 11 TO 16 FEBRUARY 1996 OVER SOUTH AFRICA[1]

2.1. INTRODUCTION

In the summer rainfall region of South Africa, the month of February 1996 represented a period of exceptionally high precipitation. The total rainfall for the month was approximately 150 to 200 per cent of the long-term average (Fig. 2.1), resulting in severe flooding in many areas of the country and in loss of life (Edwards, 1997). On the whole the summer season experienced extremely high precipitation values in agreement with the February pattern. This period did not comprise of consistently above average rainfall, but was rather the result of four extremely intense rainfall events (Edwards, 1997). The rainfall events, as identified by the South African Weather Bureau, were 20 to 29 December 1995, 16 to 27 January 1996, 13 to 17 February 1996, and 22 to 26 February 1996. Of particular interest is the event in mid-February 1996, for on this occasion widespread rains fell over almost the entire summer rainfall region. Extensive flooding and related damage was recorded, and some of the highest flood peaks of the past century were experienced (Kroese *et. al.*, 1997). The event was characterised by the interaction of a tropical low, a cold front and a ridging anticyclone. The tropical low moved into a position over the subcontinent from central Madagascar during the period 9 to 11 February 1996), and interacted with a relatively strong cold front to the south. The ridging anticyclone provided additional rainfall by directing an inflow of moisture from the east to the central reaches of South Africa.

---

[1] Manuscript authored by SJ Crimp and SJ Mason and submitted to *Meteorology and Atmospheric Physics*

Because the southern subcontinent is an arid to semi-arid region with a marked east to west decrease in precipitation (Tyson, 1986), the availability of moisture must play a key role in determining the nature and severity of precipitation events. The majority of moisture that contributes to southern African precipitation is imported from other source regions (D'Abreton and Lindesay, 1993; Mason and Jury, 1997) and so the identification of these regions is critical in determining the development and severity of such events. Macroscale vapour studies by James and Anderson (1984) have shown that the transfer of water vapour to tropical and mid-latitude regions serves to enhance the rate of growth and intensity of baroclinic systems. In southern Africa, research in this field has been limited to the investigation of mean vapour content and vapour fluxes over South Africa (McGee, 1971, 1972, 1975, 1978, 1986), the relationship between precipitable water and rainfall (Harrison, 1988) and the transport of atmospheric water vapour over the country (D'Abreton and Lindesay, 1993; D'Abreton and Tyson, 1995; D'Abreton and Tyson, 1996). Because little is known about the sources of water vapour over South Africa during summer, continued debate exists over the possible source regions. Two areas are identified as possible sources for summer rainfall, the first of which is the tropical Indian Ocean, with water vapour being advected over the continent around the South Indian Anticyclone (Tyson, 1986; Taljaard, 1986, 1987, 1990). The second area identified as a moisture source for the summer rainfall region extends southward from the tropics along the Inter-Tropical Convergence Zone (ITCZ) and Zaire Air Boundary (ZAB) (Harrison, 1986). Air flow directly from the west, from over mid- and subtropical latitudes of the Atlantic Ocean, provides minimal moisture (D'Abreton, 1996).

In this chapter, the general atmospheric conditions during the period 11 to 16 February 1996 are investigated using the Colorado State University Regional Atmospheric Modelling System (RAMS) (Tremback *et al.*, 1985). The detailed evolution of the synoptic conditions responsible for the excessive rainfall that occurred over South Africa at this time can be determined from the model simulation. The model results suggest that there were important changes in the sources of moisture through the event. A lagrangian trajectory model is used to infer the evolving nature of moisture inflow to regions that experienced the heaviest

precipitation. The trajectory model used is a modified version of that developed by D'Abreton (1996).

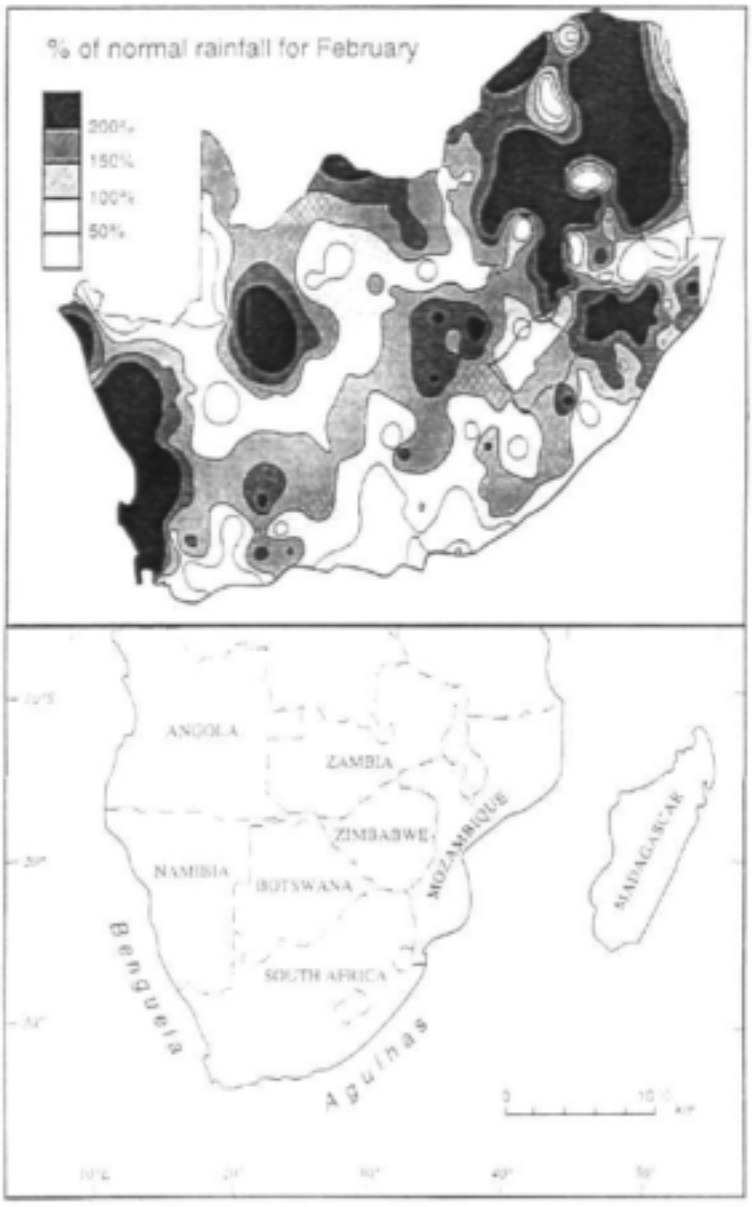

Figure 2.1. Location map of southern Africa showing the political boundaries, islands, and places mentioned in the text. The inset map of South Africa shows the 1995/96 December-February rainfall totals as percentages of the 1961-1990 average.

2.2. DATA AND METHODOLOGY

The European Centre for Medium Range Weather Forecasts (ECMWF) IIb Global Analysis data set was used in the initialisation of the atmospheric conditions for the RAMS simulation. Further initialisation is needed in the mesoscale numerical model in the form of surface data obtained from the US National Meteorological Centre (NMC), and monthly mean sea-surface temperature data from the United Kingdom Meteorological Office. RAMS is comprised of three individually developed models, two of which are hydrostatic mesoscale models (Tremback *et al.*, 1985; and Mahrer and Pielke, 1977) and the third a non-hydrostatic cloud model developed by Tripoli and Cotton (1982). As RAMS is both flexible and versatile its number of applications is varied. For this reason the modelling system contains many options for both physical and numerical processes. The model itself can be broken down into three distinct modules. The first represents the isentropic analysis stage (ISAN), where a three-dimensional atmospheric grid is created in order to moderate the boundary conditions throughout the model simulation. The second module performs the actual model simulation (MODEL) by resolving a host of numerical parameters through prescribed equations. The final module represents the visualisation and analysis module (VAN). The actual simulation process begins once ISAN has created the global isentropic grid from the ECMWF analysis data set. The domain limits are then defined in order for specific co-ordinate extraction to take place. The atmospheric variables and topography are transferred to the model domain grid by polynomial overlapping interpolation. The numerical processing is then initialised and finally the graphic output is created.

A Lagrangian trajectory model was adapted to calculate backward trajectories. Because individual trajectories can diverge fairly rapidly (D'Abreton, 1996), clusters of nine trajectories were calculated to give an indication of the uncertainties in the trajectory pathways. The trajectory model considers topographic obstacles by using a prescribed terrain-following system, and will terminate when data boundaries are reached or until the prescribed time step has been completed (D'Abreton, 1996).

The output of both RAMS and the trajectory model was analysed in order to identify the major moisture sources, and to develop a more comprehensive understanding of the structure of the atmosphere over southern Africa during this extreme rainfall event. The methodology employed involves the simulation of the period 11 to 16 February 1996 using RAMS. Variables analysed from the RAMS simulation included: *u*-, *v*-, and *w*-wind vectors; mean sea level pressure; streamlines; total mixing ratio; and accumulated convective precipitation plotted at the 146.4 m (near-surface), 3744.6 m (≈ 650 hPa), and 7406.2 m (≈ 390 hPa) levels. The 650 hPa pressure surface was chosen because it is a significant level of water vapour transport in the region (D'Abreton and Lindesay, 1993; D'Abreton, 1996). Areas of greatest precipitation were identified, and the convergence of moisture into these areas was inferred from the atmospheric flow reconstructed using the lagrangian trajectory model. The trajectory model simulation produces graphical output of latitude and longitude position, with corresponding pressure values in hectopascals (hPa) at each point (D'Abreton, 1996).

2.3. SEQUENCE OF EVENTS FROM SYNOPTIC RECORD

Satellite and synoptic information were made available by the South African Weather Bureau for the period 11 to 16 February 1996 (Fig. 2a-f). The analysis of the data showed a sequence of events producing an extremely large quantity of precipitation.

4.3.1 11 February 1996

The presence of a large tropical low situated over Botswana (Fig. 2.2a) with favourable upper level circulation produced widespread rains over the eastern half of southern Africa. The passage of a cold front and ridging anticyclone ensured heavy falls along the east coast, east of about 25°E. The predominant wind direction over the eastern half of South Africa was north-easterly, with strong onshore flow along the east coast due to the passage of the ridging high. Two other important features to note at this time were the low pressure over Madagascar, producing instability and

convective activity over the northern limits of the Island, and a coastal low developing along the west coast of the subcontinent (Fig. 2.2a).

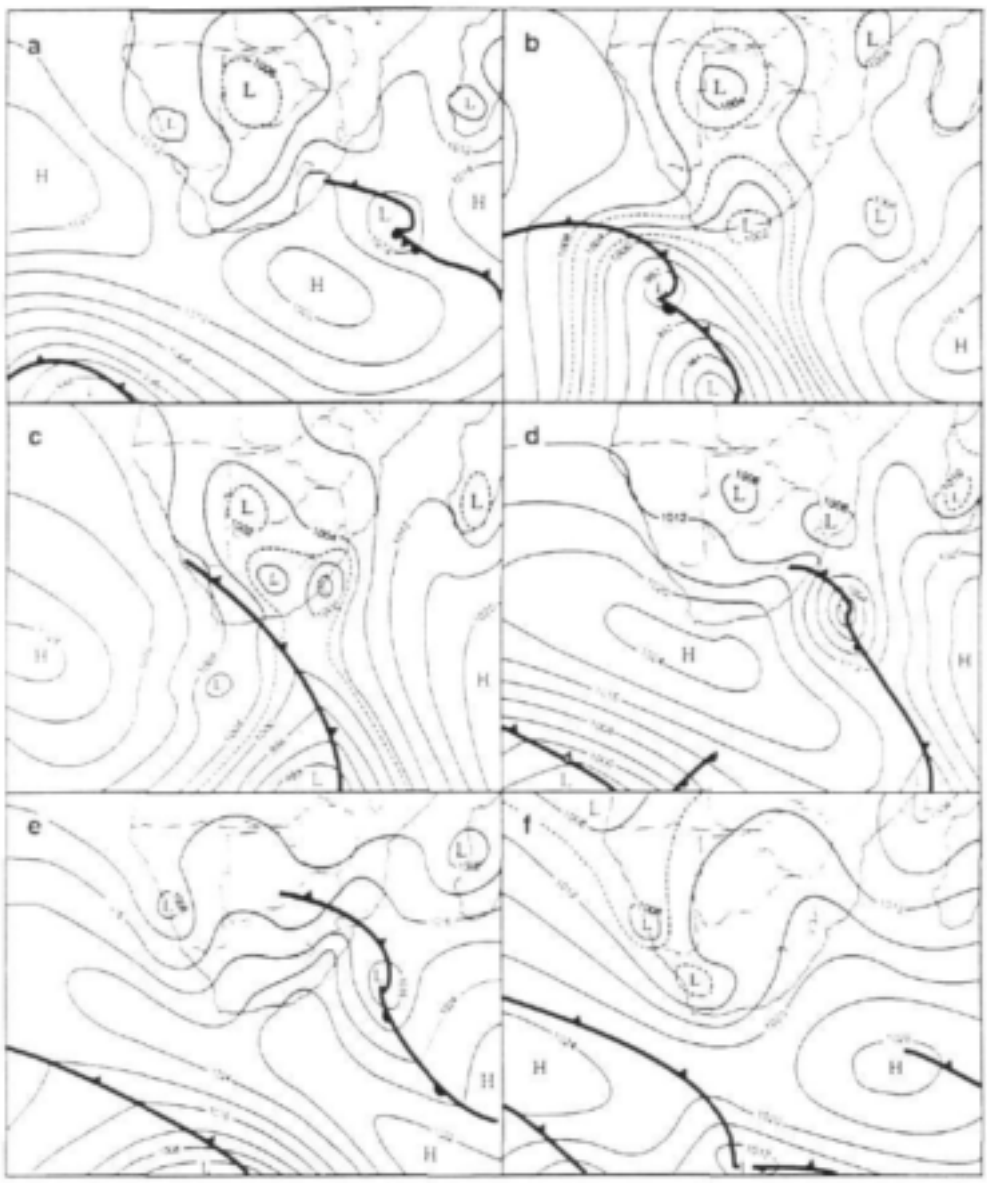

Figure 2.2. Observed sea-level pressure (hPa) at 12:00 UTC for (a) 11th, (b) 12th, (c) 13th, (d) 14th, (e) 15th and (f) 16th February 1996.

The precipitation over South Africa measured for the 24 hour period up to 12:00 UTC was widespread, with highest totals over the east coast, where falls of greater than 100 mm were experienced. Heavy rains (>90 mm) also were experienced inland in the north-eastern part of the country.

2.3.2 12 February 1996

The tropical low pressure strengthened from the previous day to 1004 hPa (Fig. 2.2b). The coastal low along the west coast filled and a second coastal low developed along the south coast ahead of the approaching cold front. The ridging anticyclone to the east of the country became entrained into the South Indian Ocean high pressure system, thus reducing the input of moisture onto, and precipitation over, the east coast of South Africa. The general wind direction over the northern region of South Africa was north-easterly, with poleward transport of latent energy along the subtropical trough. The northern regions continued to receive heavy rains, and highest precipitation values for this period were found in the northern and eastern parts of the country (>80 mm). Due to the development of a coastal low and strengthened tropical low, the south-western part of the country experienced precipitation values exceeding 45 mm, which is uncharacteristically high for a winter rainfall region.

2.3.3 13 February 1996

By 13 February the cold front had moved over the western part of South Africa (Fig. 2.2c), bringing with it widespread rains. Heavy rains and thundershowers were experienced over the eastern and central parts of the country, in association with a strengthening of the tropical low pressure. The coastal low moved along the south-east coast to about 30°E and strengthened from 1008 hPa on the previous day to 1002 hPa. Air flow at this time was predominantly meridional, having a strong southerly component on the west coast and a strong northerly component on the east coast.

Consistently high falls were a general feature over most of the country, except in the north-west and along the south coast ahead of the front. The east coastal precipitation values increased from the previous day due to the passage of the coastal low. Latent instability and thunderstorm activity were high in the northern regions of South Africa with high rainfall figures for the third day in succession. The highest recorded precipitation values were found over the central northern part of the country (>80 mm).

2.3.4 14 February 1996

During the 24-hour period between 13 and 14 February 1996, the passage of the cold front brought it to a position over the eastern half of the country (Fig. 2.2d), maintaining heavy precipitation values over this region for the fourth day in succession. The South Atlantic Anticyclone began to ridge in behind the cold front enhancing onshore flow directly behind the front (Fig 2.2d). At this time the coastal low was centred over southern Mozambique and had weakened. The tropical low over the continent had become less intense due to the intrusion of the ridging high. Heavy falls were recorded along the east coast and in the north-east (>100 mm) due to the cold air mass brought in by the ridging anticyclone, undercutting warm tropical air in circulation from the north. Over most of the country recorded rainfall was less than the previous day.

2.3.5 15 February 1996

An easterly trough began to develop over the west coast as the ridging anticyclone moved away from the country to the south-east (Fig. 2.2e). The trough was focussed at about 25°S with a central pressure of approximately 1008 hPa. The cold front that had been prevalent for the last three days continued to move towards the north-east producing widespread instability by undercutting warm moist tropical air. The combination of moisture input from the South Indian Anticyclone and the undercutting action of the cold front together with the prevalence of upper-air divergence, served to produce widespread rains over the eastern half of the country at this time. However, recorded precipitation values exhibited a marked decrease along the east coast since the previous day. Further inland, over north-eastern South Africa, precipitation values remained fairly constant.

2.3.6 16 February 1996

A further southerly extension of the west coast easterly trough occurred over the following 24 hours (Fig. 2.2f). The cold front had moved away from the country although precipitation still persisted in its wake. Precipitation was limited for the most part to the north-eastern part of the country.

2.4. MODEL SIMULATION

2.4.1 11 February 1996

At the beginning of the simulation period, a tropical low (996 hPa) was centred at approximately 20°S and 20°E (Fig. 2.3a). The South Indian (1020 hPa) and South Atlantic (1017 hPa) quasi-stationary high pressures at about 30°S were positioned a little too far south, but the anticyclonic cell (1017 hPa) ridging away from the South Atlantic high pressure was identified (Fig. 2.3a). Westerly wave disturbances to the south-west and south-east of the country were also simulated. The model did not, however, represent the coastal low or the retreating westerly low well.

High moisture concentrations and strong uplift were evident along the Mozambique Coast (0.021 $g.kg^{-1}$) and eastern South Africa (>0.016 $g.kg^{-1}$) throughout the day (Fig. 2.4). The heavy precipitation in this vicinity was apparently being fed by moisture supplied by the low level easterlies and north-easterlies around the ridging high and to the south-east of the inland tropical low. Further aloft at about the 650 hPa level, westerlies predominated over the entire country, probably supplying minimal moisture at mid-tropospheric levels (D'Abreton, 1996). However, strong uplift was facilitated by diffluent flow in the upper atmosphere.

2.4.2 12 February 1996

The simulated tropical low and subtropical trough strengthened slightly (Fig. 2.3b), as in the synoptic analysis. As a result, by mid-day there was a strong near-surface poleward flow of air simulated over much of the subcontinent (with poleward components of >16 $m.s^{-1}$) (Fig. 2.5), supplying tropical moisture to the eastern half of South Africa. Accordingly, uplift remained high along the east coast, with average near-surface values of 0.046 $cm.s^{-1}$ persisting since the previous day, and exceeding 0.25 $cm.s^{-1}$ at mid-tropospheric levels (~650 hPa). By about 21:00 UTC simulated vertical velocities at 650 hPa had increased rapidly to 0.48 $cm.s^{-1}$. Mixing ratios also increased in the region due to the heightened contribution from the tropics. Accumulated convective precipitation values showed continued heavy falls: maximum values of 10 mm in 9 hours simulated over the east coast of South Africa.

The anticyclone to the south-east of the country appeared to remain in situ a little longer than observed, with the retreating cold front displaced to the south-east and forced further from South Africa by the sublimation of the ridging anticyclone into the South Indian Anticyclone.

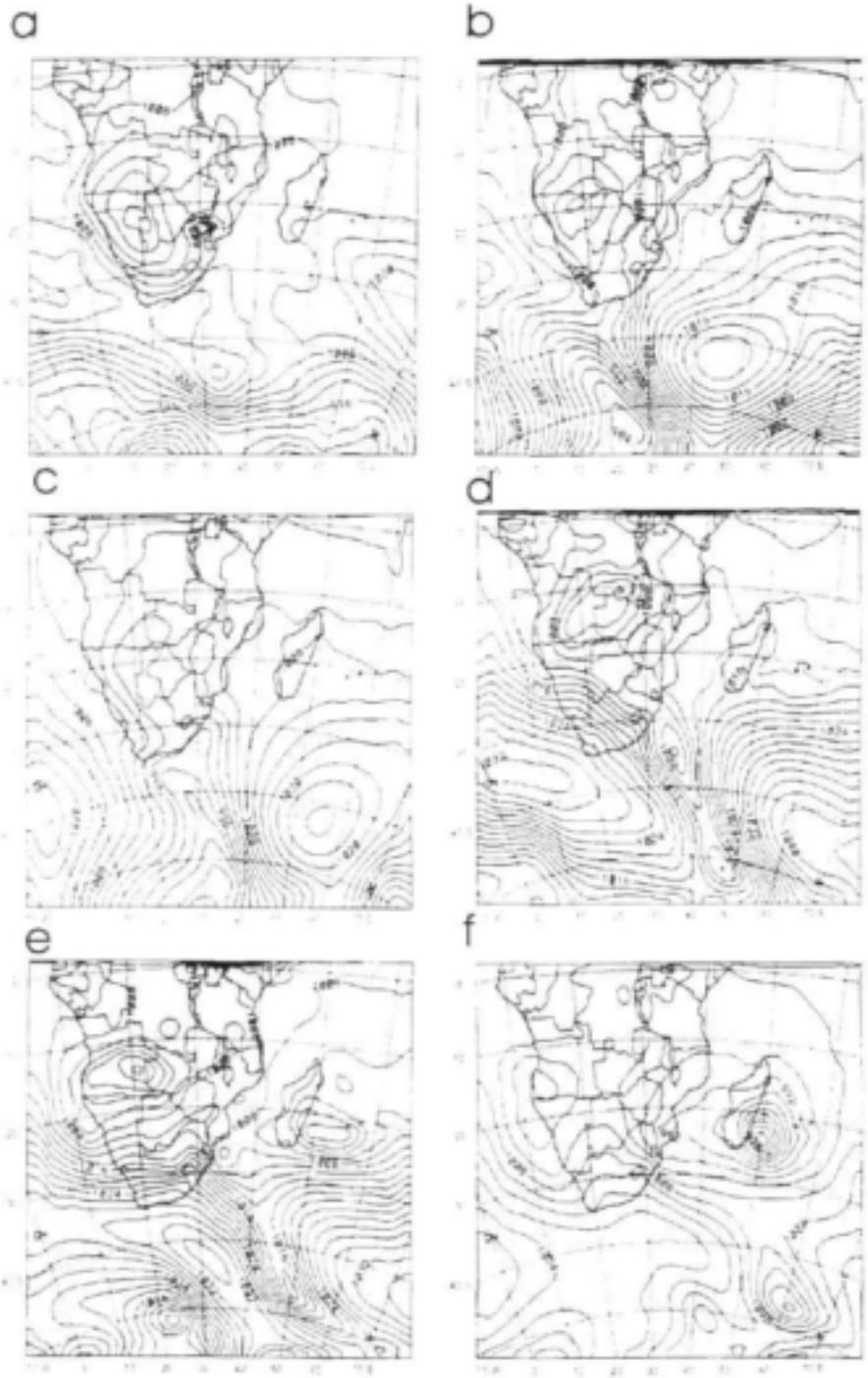

Figure 2.3. Simulated sea-level pressure (hPa) at 12:00 UTC for (a) 11th, (b) 12th, (c) 13th, (d) 14th, (e) 15th and (f) 16th February 1996 by RAMS.

Figure 2.4. Simulated near-surface (146.4 m) mixing ratios ($g.kg^{-1}\times10^{3}$) for 12:00 UTC, 11 February 1996 by RAMS. Areas with simulated mixing ratios of greater than 0.0016 $g.kg^{-1}$ are shaded.

The model only began to simulate the coastal low on the south coast late on the first day, but the approaching westerly disturbance was accurately simulated, with a central pressure as low as 982 hPa at 21:00 UTC. The approaching westerly disturbance produced increases in uplift throughout the troposphere and in precipitation south of the country along the leading edge of the cold front.

2.4.3 13 February 1996

By 13 February the simulated trough of low pressure began to align itself in a north-west to south-east position (Fig. 2.3c), consistent with the observational data. The variations in the surface pressure field simulated by the mesoscale model indicated fluctuations in the strength of the trough of low pressure with the passage of the cold front. The simulated pressure increased from 994 hPa at 00:00 UTC to 1000 hPa at

06:00 UTC. Three hours later, the pressure began to decrease steadily to 996 hPa by 21:00 UTC. The simulated position of the coastal low over the east coast was comparable to the observational data. The South Indian Anticyclone, both simulated and observed, exhibited a strong blocking action on the departing cold front. The ridging anticyclone behind the cold front was thus forced to move at a slower rate over the near coastal regions of south-western South Africa.

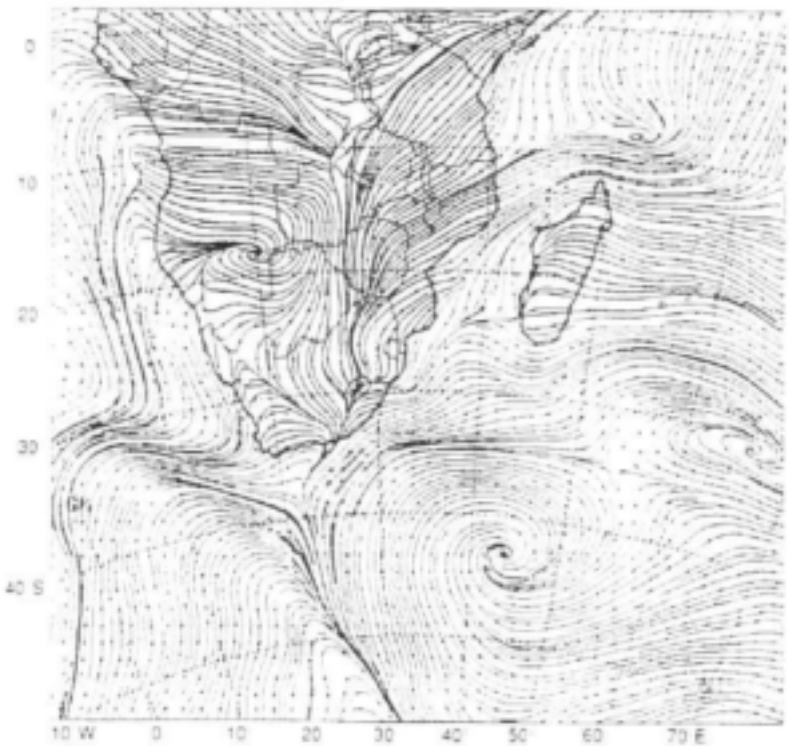

Figure 2.5. Simulated near-surface (146.4 m) streamlines for 12:00 UTC, 12 February 1996.

As the second cold front moved over the country the near-surface westerly zonal wind-components became predominant, reaching a maximum along the south coast (18 $m.s^{-1}$). A strong gradient between the westerly and easterly *u*-components developed as the progress of the cold front was reduced by the anticyclone to the east. Strong vertical ascent was simulated along the entire west coast of Namibia, and southward along the leading edge of the cold front (Fig. 2.6), where precipitation increased. Maximum near-surface vertical velocities of 0.045 $cm.s^{-1}$ were centred over the south-western part of South Africa and south of 50°S. Weaker uplift was simulated over the northern and central regions of the country (0.020 $cm.s^{-1}$). The

poleward flux of tropical air over the eastern part of the country remained strong, producing maximum total mixing ratio values (0.022 $g.kg^{-1}$) just off the east coast. With vertical velocities in the mid-troposphere remaining high into the afternoon, simulated heavy convective precipitation persisted along the east coast, with as much as 8 mm falling in 9 hours. To the north, circulation around the tropical low appeared to strengthen with developing surface convergence.

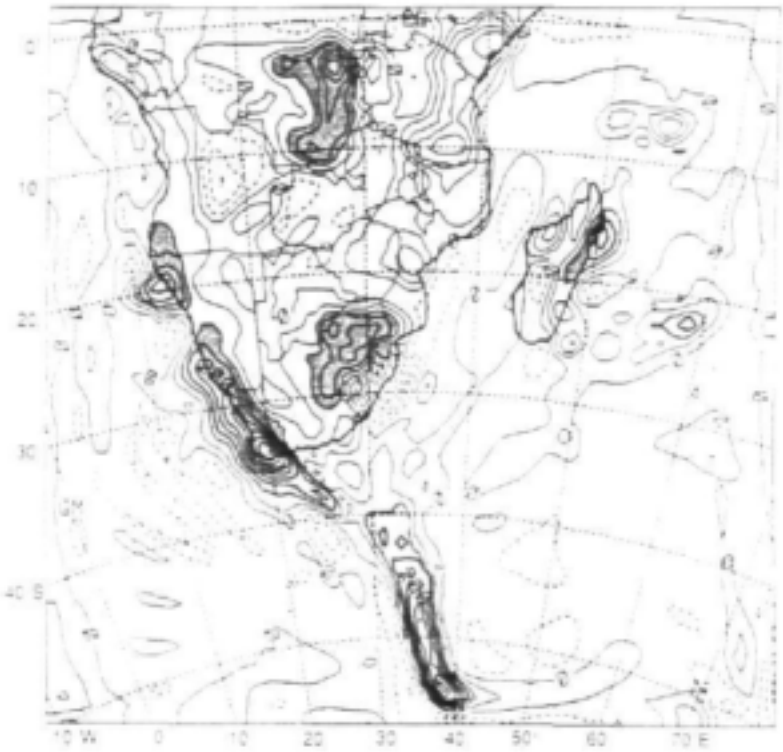

Figure 2.6. Simulated near-surface (146.4 m) vertical velocities ($cm.s^{-1} \times 10^2$) for 12:00 UTC, 13 February 1996. Areas with simulated vertical velocities of greater than +0.1 $cm.s^{-1}$ are shaded.

2.4.4 14 February 1996

The simulated westerly low moved to a position off the east coast and began to weaken (Fig. 2.3d), with the central pressure increasing from 1000 hPa at 00:00 UTC to 1012 hPa by 21:00 UTC. The model simulated the position of the South Atlantic anticyclone too far over the western half of the country, but the South Indian Anticyclone remained correctly located in relation to the south-east of the country blocking the departure of the cold front. The simulated zonal pressure gradient

between the departing cold front and the stationary high became pronounced during the course of the day with an approximately 32 hPa change in pressure over a longitudinal distance of 10 degrees (Fig. 2.3d). With the encroachment of the anticyclone from the south-west, the tropical low was displaced northward and began to weaken. The coastal low over southern Mozambique was not well-defined, but convergence into a weak tropical low began to occur over the island of Madagascar. The initiation of an easterly trough over the west coast was simulated, a little earlier than occurred in the observations.

The ridging anticyclone produced south-easterly flow over much of the country and undercut the warmer tropical air to the north. As a result, precipitation remained high over the north-eastern half of South Africa with simulated maximum values of 16 mm in 18 hours over the east coast. The pattern of vertical velocity changed quite substantially during the course of the day. Initially, vertical uplift remained pronounced along the west coast, but as the westerly disturbance advanced eastward, the region of strongest vertical uplift advanced to the southern and south-east coast (0.099 $cm.s^{-1}$ and 0.077 $cm.s^{-1}$ respectively). As the cold front moved to the east of the country, the uncoupling of the tropical and extratropical systems became evident in the streamlines. The strength of the convergence over Angola and Zambia was enhanced as the system decoupled, with air flow becoming predominantly zonal between 10°S and 20°S.

2.4.5 15 February 1996

The model simulation continued to plot the slow movement of the westerly disturbance away from the country with a cell of anticyclonic circulation ridging in very close behind (Fig. 2.3e). The disturbance became isolated from the continent by the continued eastward extension of the ridging high. The weak low pressure simulated on 14 February over the island of Madagascar developed rapidly during the course of the day from 1008 hPa at 00:00 UTC to 990 hPa by 21:00 UTC. The developing convergence over Madagascar resulted in a westward and south-westward expansion of the westerly *u*-components from north of Madagascar, from the previous day. By 18:00 UTC the westerly component reached 12 $m.s^{-1}$ in the Mozambique

Channel. However, the air flow over South Africa remained predominantly south-easterly due to the ridging action of the high pressure system.

Localised mixing ratio maxima were simulated in the southern Mozambique Channel (0.021 $g.kg^{-1}$), and west of Namibia (0.023 $g.kg^{-1}$) (Fig. 2.7). The moisture availability over the Indian Ocean, south of Madagascar, allowed the rapid growth of the tropical low in the region. The simulation of anomalously high mixing ratio values over the Atlantic Ocean took place due to the simulated westward movement of the tropical low. The circulation of the low facilitated the transport of moisture from a region near the equator to the Atlantic Ocean. Accumulated convective precipitation values for 15 February showed a concentration of heavy falls in the southern Mozambique Channel and south of Madagascar, where maximum falls of 24 mm in 18 hours were simulated.

2.4.6 16 February 1996

The easterly trough over the west coast that had been simulated for the past two days became well-defined and showed signs of intensification (Fig. 2.3f), providing high vapour mixing ratio values to the region. The ridging anticyclone remained in circulation over most of the country, feeding moist air over the continent from the adjacent Indian Ocean. Simulated precipitation values therefore remained high along the east coast. Strongest precipitation occurred to the south of Madagascar, however, in association with the tropical low. This low intensified rapidly from 987 hPa at 00:00 UTC to 960 hPa at 12:00 UTC. Strong vertical ascent (0.11 $cm.s^{-1}$) was simulated and mixing ratio values intensified dramatically. The retreating westerly disturbance was positioned well to the south-east of the country (Fig. 2.3f).

2.4.7 Summary

On the whole the model simulation of the analysis period 11 to 16 February 1996 corresponded well with the synoptic and precipitation data supplied by the South African Weather Bureau. The model output showed some discrepancies in the strength and position of some of the synoptic features and an inability to simulate coastal features adequately, but the evolution of the main features was reproduced accurately.

Figure 2.7. Simulated near-surface (146.4 m) mixing ratios ($g.kg^{-1}\times10^{3}$) for 12:00 UTC, 15 February 1996 by RAMS. Areas with simulated mixing ratios of greater than 0.0018 $g.kg^{-1}$ are shaded.

From a simple analysis of the simulated synoptic conditions, it seems that there were a number of evolving moisture sources during the six-day period. Over the eastern part of the country, moisture was apparently supplied from tropical latitudes on the 12th and 13th, and by low-level easterlies and south-easterlies during the rest of the period. As the easterly disturbance to the north of South Africa became decoupled from the westerly disturbances to the south on the 14th, it moved slowly westward and may have diverted tropical moisture to the Atlantic coast. At the same time, the development of the tropical disturbance near Madagascar resulted in convergence of tropical moisture there from the 15th. It therefore seems unlikely that there was a large input of tropical moisture over South Africa some time after 14 February. Over the south coast and south-western part of the country, the cold fronts were responsible for some heavy rains. Details relating to the evolving moisture sources were inferred using backward trajectory analysis, as discussed in the following section.

2.5. Trajectory Analysis

Clusters of ten-day backward trajectories were calculated with initial points centred over the east coast (29°S, 32°E), the northern interior (23°S, 30°E), and the south-west Cape (34.5°S, 21°E). The backward trajectories were used to infer the evolution of moisture pathways over the period 11-16 February 1996. These sites were selected because significant volumes of rainfall occurred in their vicinity during the period.

2.5.1 East Coast

Over the east coast (29°S, 32°E), low-level flow (950-850 hPa) at first originated from the south-east. Most of the trajectory parcels had remained almost stationary near the surface over the warm Agulhas Current, although there was also some recirculation around the South Indian High onto the coast (Fig. 2.8). Approximately five days earlier, this air mass off the east coast formed part of the westerly flow, and was descending slowly from above 700 hPa. Above about 700 hPa, the backward trajectories exhibited a strong westerly pattern directly over the continent from the Atlantic Ocean. Presumably the low-level flow from over the south-west Indian Ocean had had time to evaporate sufficient moisture from the underlying ocean, which supplied the moisture for the east coast.

Trajectories run from 12 February highlight the strong influence of the ridging anticyclone on the lower atmospheric levels below 850 hPa. The trajectory parcels reaching the east coast had again originated in the westerlies, but at levels below 850 hPa. They followed a pathway directly northward over the three days up to 12 February, due to the proximity of the ridging anticyclone and the passage of a cold front. Above 850 hPa the westerly flow once again predominated, although at levels higher than about 600 hPa evidence of continental recirculation existed: the air had originated from over Botswana and Namibia (Tyson, 1997). A similar pattern persisted on 13 February, whereby low-level inflow was again originally from the westerlies, recurving over the warm south-west Indian Ocean and reaching the east coast from the south and south-east. Above 800 hPa, westerly flow remained

dominant, and it was only above about 600 hPa that there was evidence of a tropical origin.

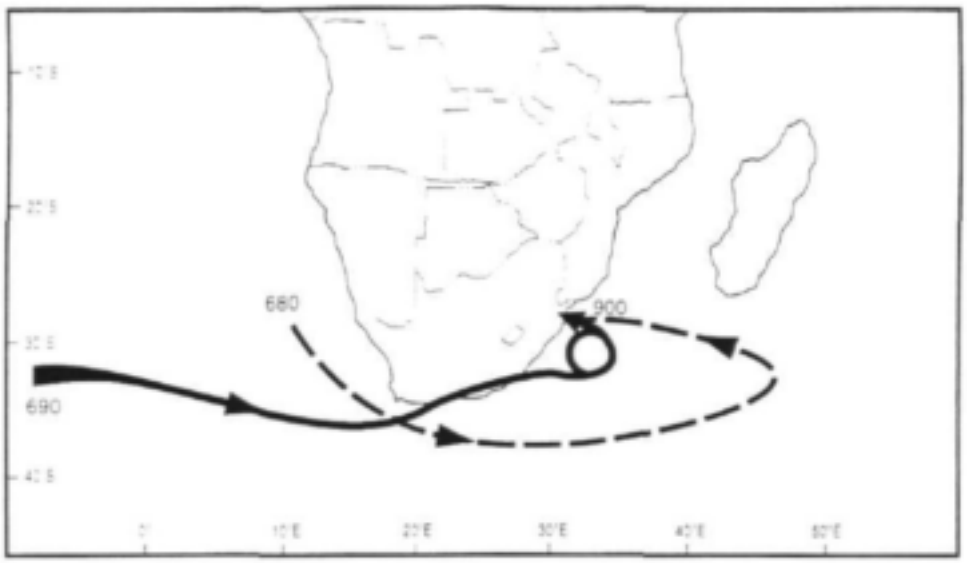

Figure 2.8. Ten-day backward trajectory clusters from a point centred over the east coast (29°S, 32°E). The trajectories were initiated at 12:00 UTC on 11 February 1996 at 900 hPa.

By 14 February the origin of low-level air converging over the east coast began to change. Although at near-surface pressure levels (below about 900 hPa) the predominant westerly flow into the Indian Ocean with characteristic south-easterly recurve onto the east coast still predominated, there was some evidence for input from the east of Madagascar. Between the 850 and 700 hPa levels, this easterly flow onto the east coast was the dominant trajectory pathway (Fig. 2.9). Above 700 hPa the continental recirculation was again evident up to about 550 hPa, above which ascending easterly flow would have provided a source of mid-tropospheric moisture. On 15 February the near-surface easterlies originating from east of Madagascar became the main source due to the passage and proximity of a cold front and because of the influence of the South Indian Anticyclone. The easterlies extended up to at least the 500 hPa level. Low-level easterly inflow around the large ridging anticyclone located to the south-east continued to occur on 16 February. Above the 800 hPa level, however, recurved westerly flow became evident, but the ascending easterly flow persisted above 550 hPa.

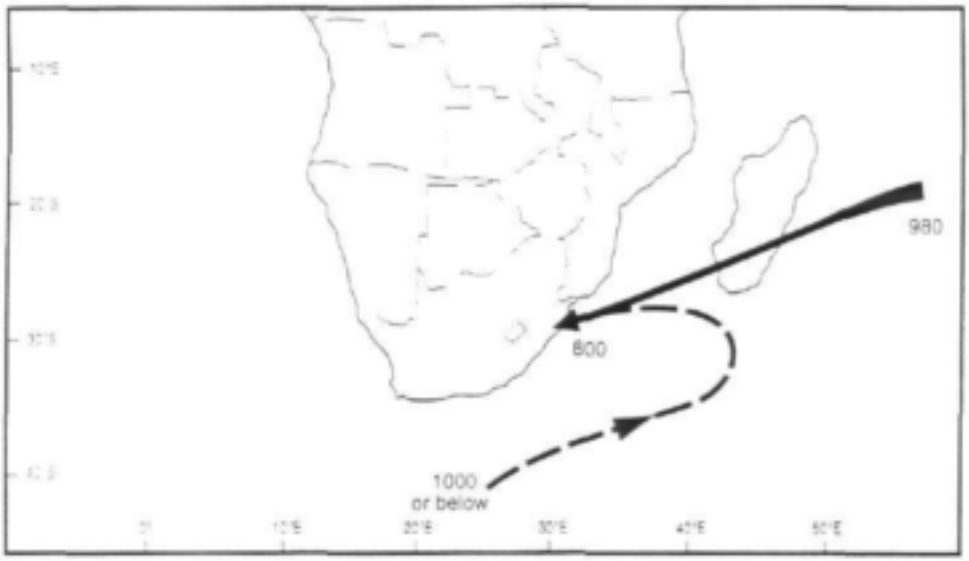

Figure 2.9. Ten-day backward trajectory clusters from a point centred over the east coast (29°S, 32°E). The trajectories were initiated at 12:00 UTC on 14 February 1996 at 800 hPa.

2.5.2 Northern Interior

For the northern interior (23°S, 30°E), the predominant influence on the trajectory pathways for 11 February was the proximity of the ridging high pressure system east of South Africa and its passage over the previous days. Low-level flow (below 800 hPa) reaching the northern interior on the 11th originated over the southern Indian Ocean and not over the Atlantic Ocean as for the east coast. Between the 800 and 700 hPa levels, continental recirculation predominated. Above 700 hPa localised recirculation occurred above the northern interior.

On 12 February the near-surface pattern remained relatively unchanged from the previous day with the main trajectory pathways showing recirculation of the westerlies over the Indian Ocean around the succession of ridging anticyclones (Fig. 2.10). This pattern was prevalent below the 750 hPa pressure level with a greater westerly component with increasing altitude. Between 750 and 650 hPa the trajectory pathways were almost entirely continental with strong localised recirculation over many parts of South Africa. Above the 650 hPa level the trajectories followed a westerly pathway directly over the continent. The inflow of air on the 13th was very

similar to the previous day: low-level air originated from ocean areas to the south-east, while higher up, westerly flow became evident.

As over the east coast, by 14 February the origin of air converging over the northern interior became the area to the east of Madagascar. Below 850 hPa the inflow was mainly from the south-east, but between 850 and 700 hPa ascending air from the east was predominant (Fig. 2.11). Ascending tropical air also occurred above 600 hPa, originating from the continental interior. The ascending easterly and south-easterly flow persisted on 15 and 16 February below the 650 hPa level. Above 700 hPa, some descending westerly flow was apparent. This convergence of descending westerly and ascending easterly flows producing heavy rainfall over the country is consistent with the results of D'Abreton and Tyson (1996).

2.5.3 South-west Cape

Over the south-west Cape (34.5°S, 21°E), near-surface trajectory pathways for 11 February indicate localised recirculation over the western half of South Africa with limited westerly input (Fig. 2.12). Between the 850 and the 700 hPa pressure levels, easterlies dominated the overall pattern of air flow into the region. The trajectories between these pressure surfaces travelled at a constant level, with limited vertical ascent or descent. Above 700 hPa, air flow was exclusively from the west, again with limited vertical motion. This pattern of air flow was broadly similar on 12 February, although the near-surface flow was more distinctly westerly than on the previous day, and the easterly inflow below 700 hPa was less dominant. The easterly mid-level inflow (between 850 and 700 hPa) was re-established on 13 February, this time recirculating from the north and east (Fig. 2.13). Vertical motion in this flow was weak, but undercutting by the near-surface flow from the west resulted in frontal rain. Above 700 hPa, westerly inflow predominated. On 14 February, the easterly mid-level flow that had provided much of the moisture for the rainfall over the south-west Cape started to become less dominant. By the 15th, the westerlies were prevalent throughout the atmospheric column, and this pattern persisted into the following day.

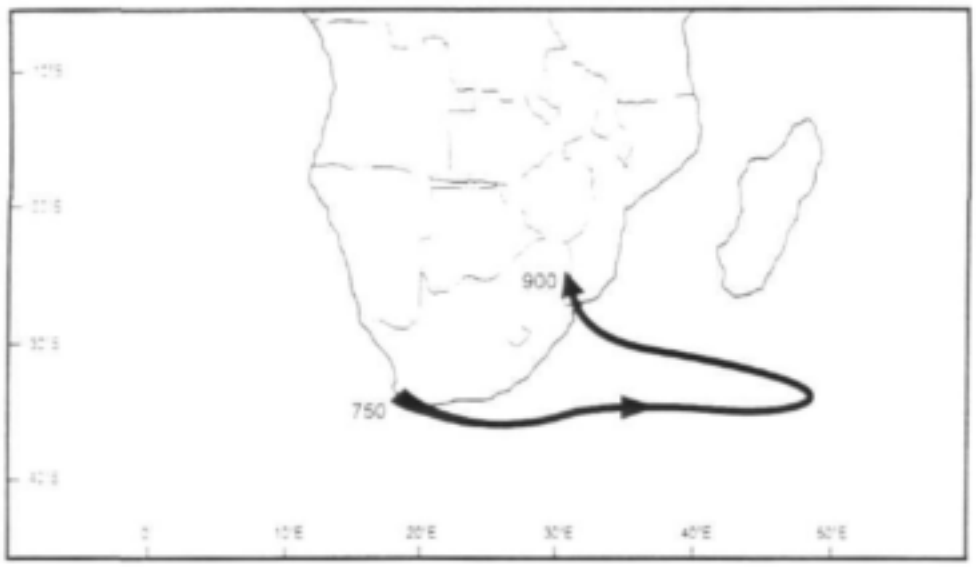

Figure 2.10. Ten-day backward trajectory clusters from a point centred over the northern interior (23°S, 30°E). The trajectories were initiated at 12:00 UTC on 12 February 1996 at 900 hPa.

2.5.4 Discussion

On 11 February 1996, the departing cold front and ridging anticyclone produced an import of warm, moist air over the eastern part of the country from the south-west Indian Ocean. On penetrating the interior the onshore flow became entrained in the flow pattern of the developing tropical low pressure system over Botswana. Above the near-surface, however, strong westerly *u*-components predominated over the country. This relatively cold, dry air aloft together with the warm, moist near-surface inflow would have been responsible for the strong instability along the east coast. Uplift of the near-surface layer, and the release of instability, was initiated by the topographic effects of the air moving inland, and was propagated by diffluent flow in the upper atmosphere.

The tropical low situated over Botswana strengthened on 12 February and a subtropical trough linked the system with a westerly disturbance to the south of the country. Despite the resulting poleward flow, the source of low-level moisture was ultimately from the south-east. The inland low provided the pressure gradient to maintain the convergence of air and moisture over the land, resulting in persisted

heavy rainfall over the eastern part of South Africa. Westerlies in the mid-troposphere and diffluent flow aloft continued to provide sources of instability, although some evidence of mid-tropospheric tropical air was identified and would have provided additional moisture.

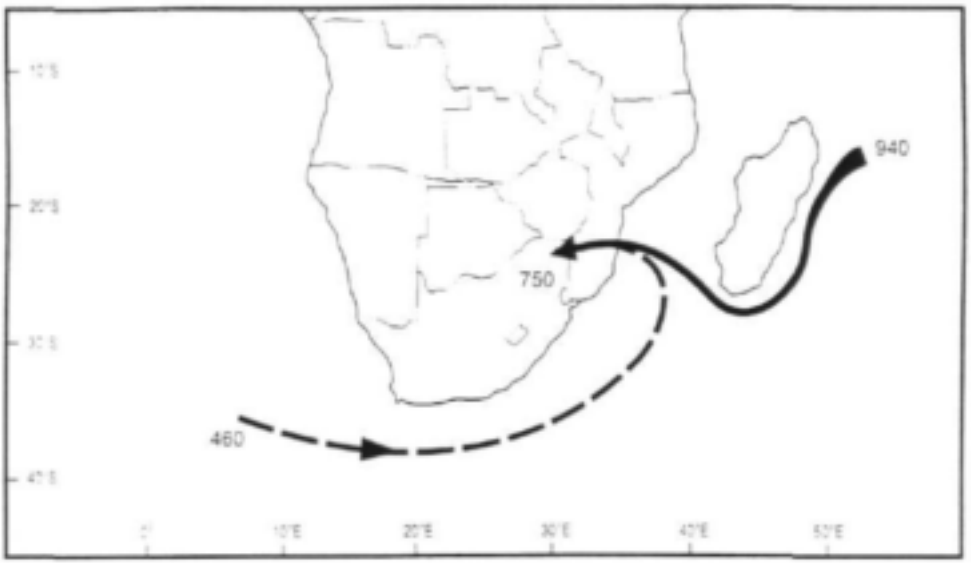

Figure 2.11. Ten-day backward trajectory clusters from a point centred over the northern interior (23°S, 30°E). The trajectories were initiated at 12:00 UTC on 14 February 1996 at 750 hPa.

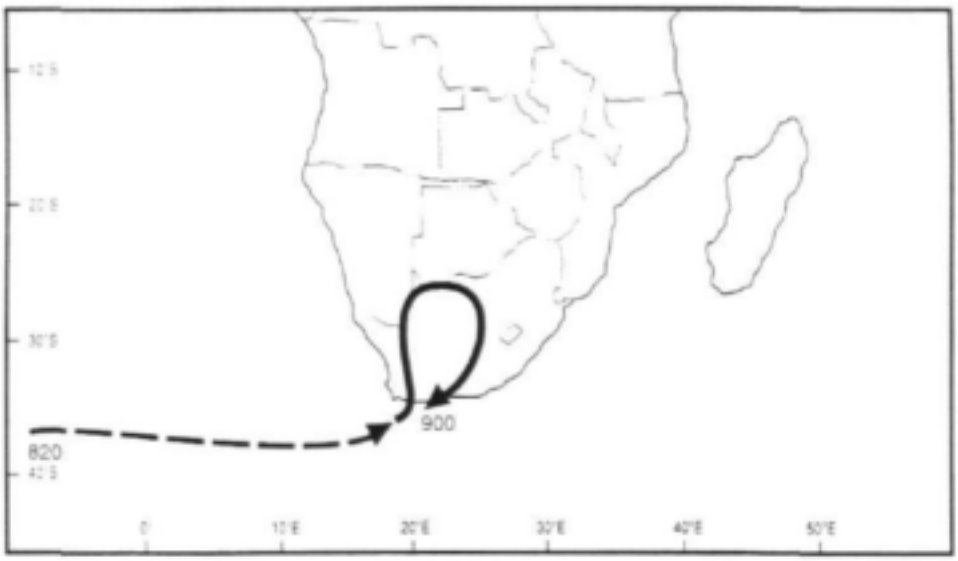

Figure 2.12. Ten-day backward trajectory clusters from a point centred over the south-west Cape (34.5°S, 21°E). The trajectories were initiated at 12:00 UTC on 11 February 1996 at 900 hPa.

On 13 February 1996 the synoptic circulation pattern showed the landfall of the cold front approaching from the south-west. The front provided heavy rainfall to the south-western part of the country, which usually receives rainfall only in winter. The cold descending westerly air in the rear of the front undercut easterlies in the mid-troposphere that had imported moisture from the Indian Ocean. Convergence of moisture into coastal low on the 13th and 14th provided the continued heavy rains over the eastern part of the country. Moisture was now being supplied from areas directly to the east, rather than the south-east.

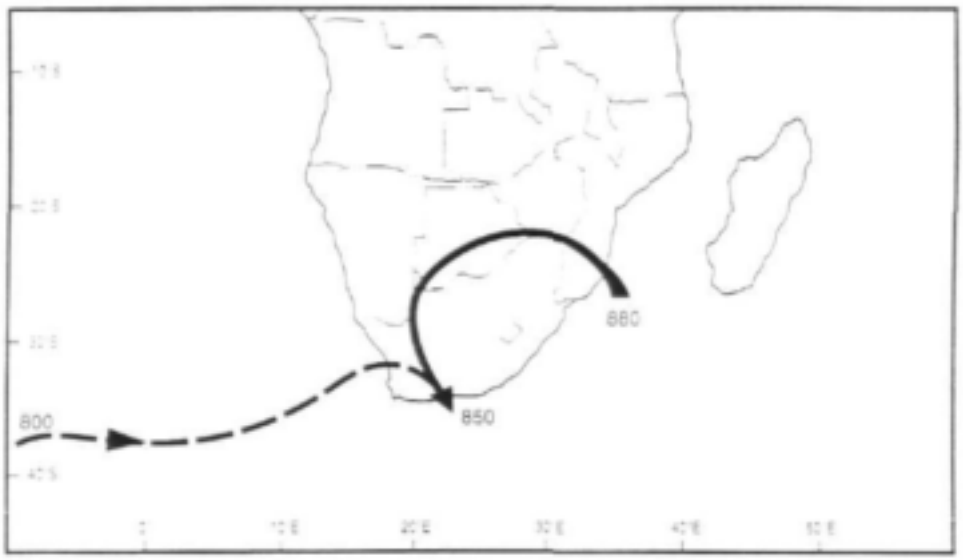

Figure 2.13. Ten-day backward trajectory clusters from a point centred over the south-west Cape (34.5°S, 21°E). The trajectories were initiated at 12:00 UTC on 13 February 1996 at 850 hPa.

By 14 February 1996 the cold front had moved over the eastern half of the country with a ridging high developing behind. The tropical low pressure and cold front decoupled, resulting in a reduction in vertical ascent along the cloud band. Heavy precipitation was now limited to the eastern coastal regions. Over the eastern part of the country, mid- to low-level moisture was supplied from east of Madagascar by the South Indian Anticyclone. This moisture source persisted over the next two days, providing heavy rains to the eastern half of the country.

2.6. CONCLUSIONS

The combination of mesoscale numerical modelling and trajectory analysis of the extreme rainfall period from 11 to 16 February 1996 over South Africa has proved a useful tool in the analysis of both mesoscale atmospheric circulation and the identification of important moisture pathways. The general circulation for the period 11 to 16 February is well modelled with the RAMS regional scale numerical model and creates a three-dimensional perspective not available before. The trajectory model provides a useful depiction of parcel transport, giving an indication of possible moisture sources throughout the analysis period.

Initially, the moisture source for the event was the south-west Indian Ocean. Recurved westerlies to the south of the country were forced over the warm Agulhas Current inland by a ridging anticyclone and a tropical low over Botswana. Uplift was forced by topography and was facilitated by strong instability caused by cold westerlies in the mid-troposphere and diffluent flow in the upper-troposphere. The easterly supply of moisture became increasingly dominant after 14th February when most moisture originated from north of 30°S. The streamlines calculated by the RAMS model suggested that tropical moisture was an important source on 12th and 13th February when the tropical low over Botswana was coupled with a westerly disturbance to the south. The trajectory analysis, however, suggests that the snapshot image provided by the streamlines is misleading; there is a lag of one or two days before the tropical moisture reaches South Africa. Of particular interest is the absence of a significant moisture supply from tropical areas to the north, or from the equatorial Indian Ocean. Presumably the development of the west coast trough and the tropical low over Madagascar diverted the tropical moisture away from the country. Apparently, given favourable synoptic conditions, significant rainfall events can occur over South Africa with moisture supplied from the subtropical latitudes of the Indian Ocean. The commonly held premise that atmospheric moisture is predominantly derived from the equatorial Indian Ocean during extreme rainfall events over South Africa appears to be inaccurate. For the duration of the event of 11-16 February 1996, the subtropical Indian Ocean to the south and east of Madagascar provided moisture for the continued genesis of precipitation. Research of this nature must continue in order to determine if

moisture sources for rainfall over South Africa are event-specific or indeed are derived predominantly from the equatorial Indian Ocean.

CHAPTER 3

ENSEMBLE SEASONAL FORECASTS OF JANUARY-APRIL 1996 RAINFALL OVER SOUTHERN AFRICA BY THE UNITED KINGDOM METEOROLOGICAL OFFICE

3.1. INTRODUCTION

Since the 1995/96 rainfall season, the UKMO have been releasing seasonal forecasts for southern Africa using their Unified general circulation model. The model does provide predictability of winter and spring mean sea-level pressure and 500 hPa surface heights over the North Atlantic - European sector (Davies *et al*, 1997). The predictability in this region results, in part, from the predictability of the North Atlantic Oscillation given strong sea-surface temperature anomalies. Since rainfall over southern Africa is known to respond to strong sea-surface temperature forcing in the Pacific and Indian Oceans, and to a lesser extent the Atlantic Ocean (Mason and Jury, 1997), some predictability of southern African rainfall may be evident.

In September 1995, statistical models were predicting above average rains for the period up to December. Similarly, the UKMO Unified model ensemble forecast produced in September indicated above average rains for the same period. However, some of the statistical models and the UKMO ensemble forecast issued in January indicated average or below average rains for the second half of the rainfall season. Ensemble mean forecasts for most of South Africa were for average conditions, but dry conditions were forecasted for the north-east of the country and for the rest of the subcontinent south of about 5°S (Figure 3.1). Exceptionally good rains were received over much of southern Africa during the second half of the 1995-96 season, with widespread flood conditions in February. Similarly, during the 1996-97 season, the UKMO model was indicating dry conditions in the second half of the season, whereas good rains fell in March. Apparently, the operational performance of the model is

worse for the second half of the season than for the first, whereas the inherent predictability of the atmosphere over southern Africa is greatest for the second half of the season (Mason *et al*, 1996).

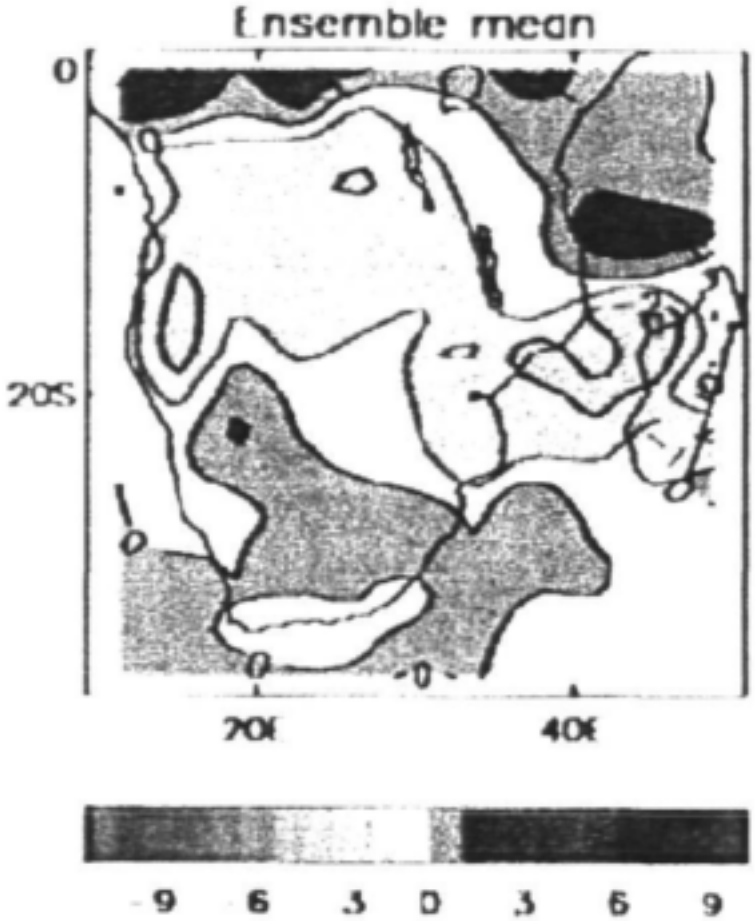

Figure 3.1: Ensemble mean rainfall anomaly forecasts for January to April 1996 from the United Kingdom Meteorological Office. Units are in mm per day.

In this Chapter, the UKMO ensemble forecast released in January 1996 for the second half of the 1995-96 rainfall season is compared with observational data obtained from ECMWF. The differences in the atmospheric circulation and inferred moisture fluxes between the ensemble members and the observations are examined and possible reasons for the failure of the model are discussed.

3.2. DATA AND METHODS

Backward Lagrangian trajectories were calculated from ECMWF data and the ten UKMO time-lagged ensemble member forecasts for each day during the period 11 January to 30 April 1996. The UKMO ensemble members were initialised on successive days beginning 23 December 1996. The trajectories were calculated using a three-dimensional Lagrangian trajectory model and were started at 800, 750 and 700 hPa from a nine-point grid, spaced at 1° of latitude and 1° of longitude and centred over Johannesburg (26°S, 28°E). The trajectory model is a fully revised version of that developed by D'Abreton (1996).

The number of times a trajectory crossed a line of longitude in an easterly or a westerly direction was counted and expressed as a percentage of the total number of trajectories. The analysis was repeated for northerly and southerly transport across lines of latitude. Major pathways of trajectories were then determined and were confirmed by visual inspection of the individual trajectories.

3.3. RESULTS AND DISCUSSION

The main trajectory pathways of air over Johannesburg from the ECMWF data and the UKMO model seasonal forecast are indicated for the months of January to April 1996 in Figure 3.2. Easterly zonal transports constituted the largest component and percentages are shown in the Figures. Percentages of westerly transport are also shown by the progressive dotted fill. Meridional transport is indicated by the arrows, but is not shown by contours.

Although there are a number of encouraging similarities between the main trajectory pathways of the observations (ECMWF data) and the seasonal forecast (UKMO model output), there are some noticeable differences that would indicate possible causes for the failure of the forecast. There is an absence of northerly transport by the UKMO ensemble members and the percentages of easterly transport by the UKMO

ensemble members are consistently too high: there is more variability in the ECMWF data.

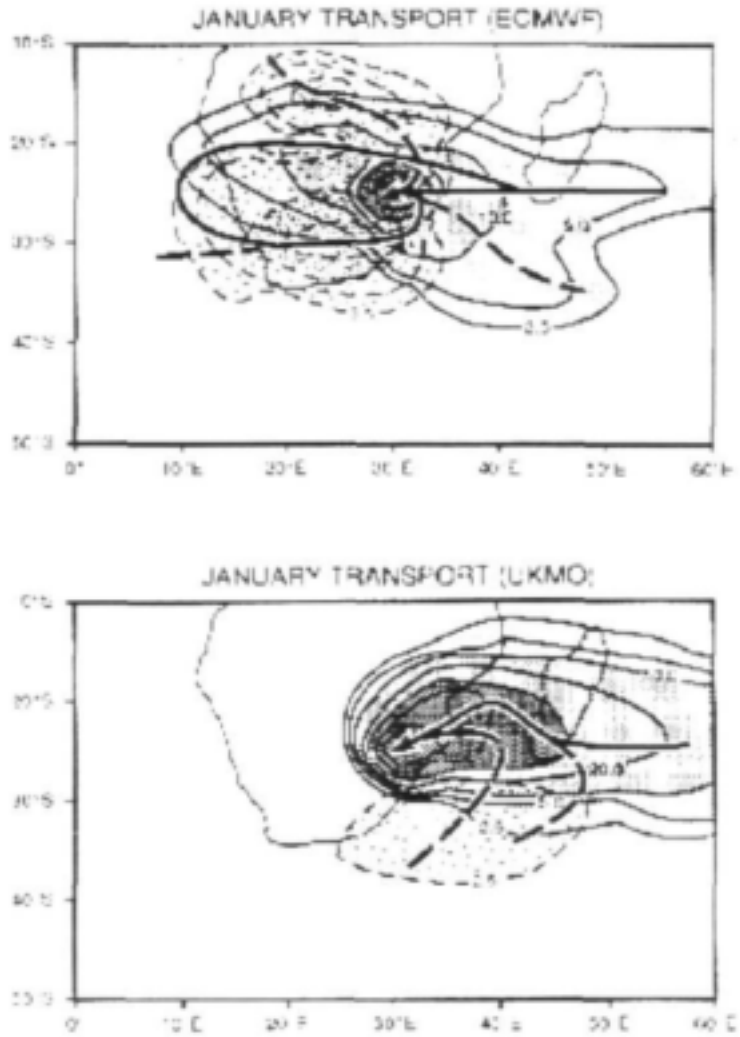

Figure 3.2: The primary (solid arrows) and secondary (dashed arrows) air transport into an area centred over Johannesburg (⊕) calculated using 10-day backward trajectories. The percentages of trajectories travelling in easterly directions (contoured at intervals of 2,5, 5,0, 10,0, 20,0, 30,0, 40,0 and 50,0%, shaded). The percentages of westerly transports (dashed contours, dotted shading). The backward trajectories start at 800, 750 and 700 hPa and from a nine-point grid, spaced at 1° of latitude and longitude and centred over 26°S, 28°E. The percentages for the UKMO Unified Model are for all ten ensemble members.

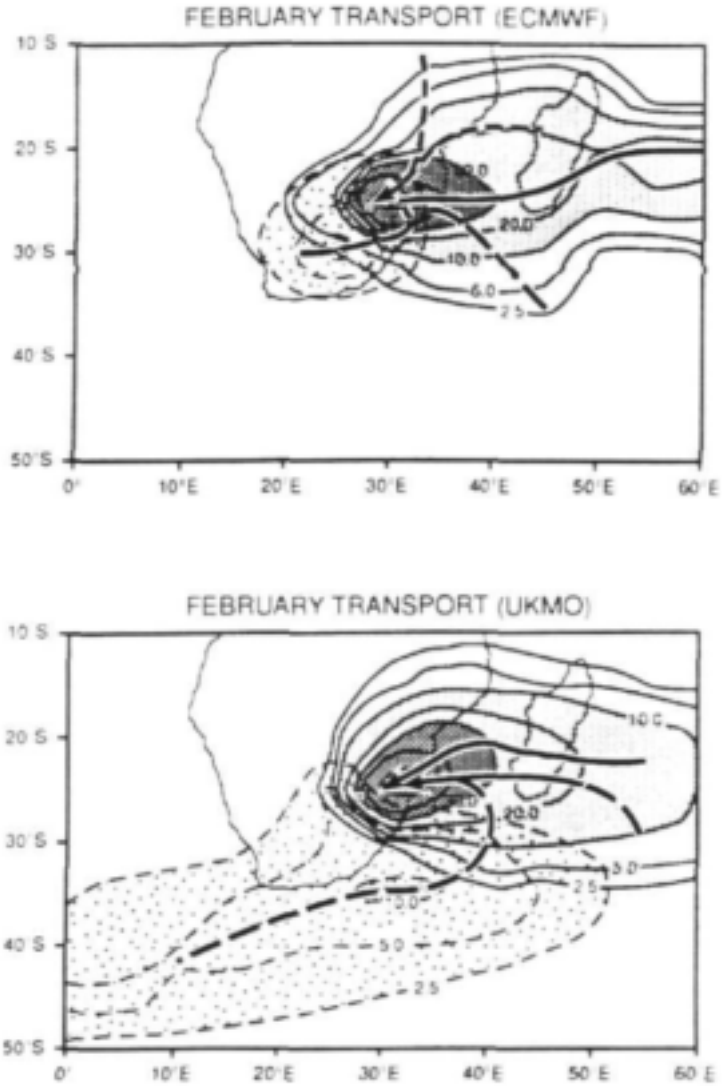

Figure 3.2: Continued.

However, the most important difference is that the northward expansion of the westerlies during February in the UKMO ensemble member forecasts occurs too early. The gradual northward expansion of the westerlies is evident in both the UMKO forecasts and the ECMWF data with the progression of the season and is consistent with the reduction of rainfall toward April. The westerlies are known to bring relatively cold, dry air to southern Africa. Most moisture that is eventually precipitated over southern Africa during the second half of the rainfall season (January onwards) is believed to originate from the tropical western Indian Ocean

(D'Abreton and Lindesay, 1993; D'Abreton and Tyson, 1995). The flood-producing rains of January and February 1996 have been associated with the southerly transport of moist tropical air over the subcontinent. The early onset of the westerlies in the UKMO model may therefore be partly responsible for the disappointing performance of the forecasts. If so, the model may be inherently unable to provide skilful forecasts of the second half of the rainfall season since strong westerlies over South Africa are a feature of the control climate of the model (Joubert, 1997).

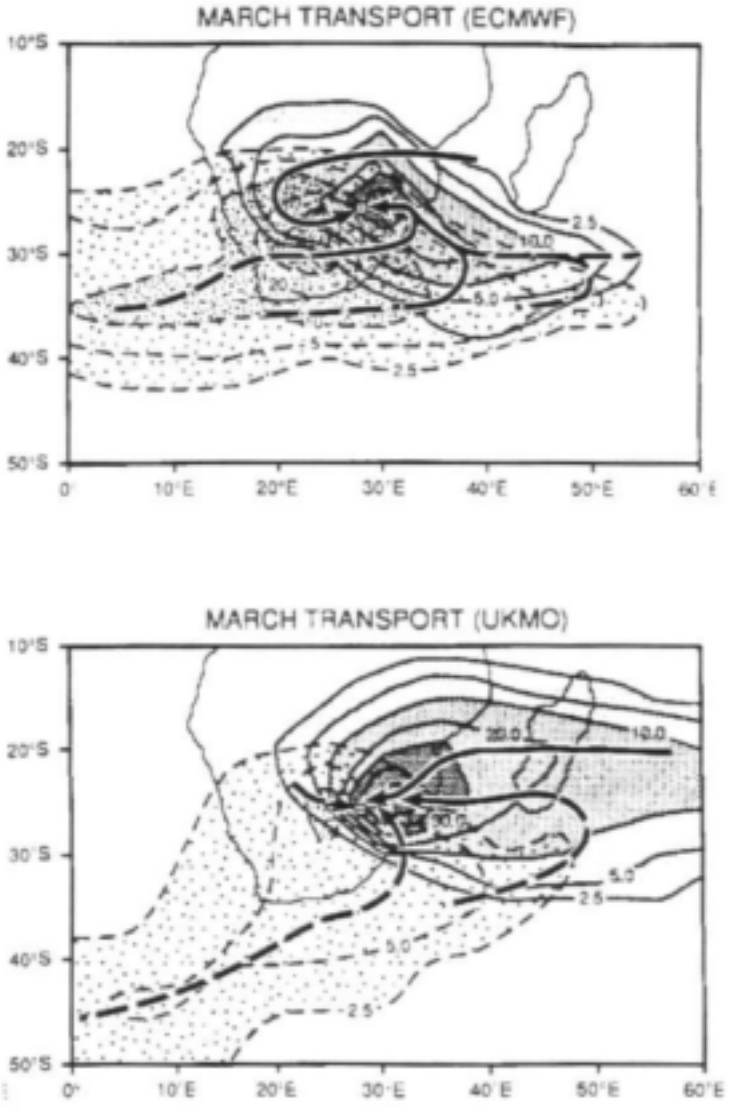

Figure 3.2: Continued.

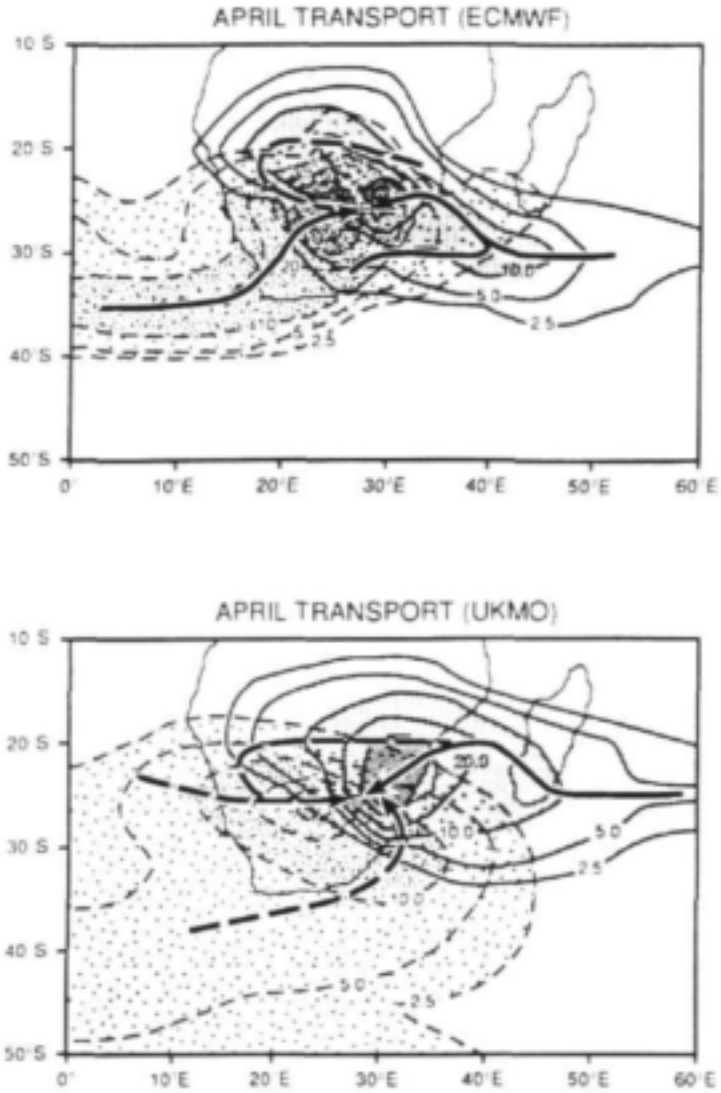

Figure 3.2: Continued.

3.4. SUMMARY

A seasonal forecast for southern African rainfall for the period January - April 1996, that was released in early January by the United Kingdom Meteorological Office, suggested that conditions would be dry over much of the subcontinent north of South Africa, and close to average over South Africa itself. Flood conditions were experienced. The failure of the general circulation mode to indicate wet conditions may be related to a limitation in the model's control climate: the northward

progression of the westerlies during autumn occurs too early and effectively results in a premature end to the rainfall season. As a result, the model may be inherently unable to produce reliable seasonal forecasts for the second half of the season. The causes of this model-limitation deserve further investigation and may result in significant improvements in forecast skill if the problem can be resolved. The model seems to have performed reasonably well for the first half of the season, when the atmosphere is actually inherently less predictable. Detailed diagnosis of the early season rainfall forecasts is warranted.

CHAPTER 4

AIR MASS TRANSPORT AND ASSOCIATED MOISTURE SOURCES DURING CYCLONE DEMOINA, JANUARY 1984[1]

4.1. INTRODUCTION

Although much of southern Africa is semi-arid, its climate is marked by pronounced spatial and temporal variability, and it is not uncommon for extreme rainfall events to occur (Triegaardt, 1963; Triegaardt *et al.*, 1991; Lindesay and Jury, 1991, D'Abreton and Lindesay, 1993; D'Abreton and Tyson, 1995). The impact of these extreme events can be severe, with associated floods causing damage to property, loss of life and disruption to economic activity. Tropical cyclones infrequently affect the southern African region, but the economic and social costs of such storms is great. Currently, the ability to forecast accurately which of these systems will persist and influence the eastern regions of subtropical southern Africa is limited, due to an incomplete understanding of the sources of moisture and air mass transport associated with such intense weather systems.

A Lagrangian trajectory model has been successfully utilised for determining air mass transports over southern Africa (D'Abreton, 1996; D'Abreton and Tyson, 1996, Tyson *et al.*,1996a; Garstang *et al.*, 1996; Tyson, 1996b), thus enhancing existing knowledge about the structure of specific rain-bearing systems. A trajectory analysis of the cut-off low system which resulted in devastating floods over Laingsburg during January 1981 identified a complex of three-dimensional conveyors representing different air masses and the interaction of variable moisture source regions (Van den Heever, 1995; D'Abreton and Tyson, 1996). The approach has not yet been applied to case studies of tropical cyclones over southern Africa.

---

[1] Manuscript co-authored by SJ Crimp, AM Joubert and W Tennant, and submitted to *Water SA*.

Although tropical cyclones seldom reach South Africa, they often track down the Mozambique Channel and impact on neighbouring countries. In the last forty years eleven tropical cyclones have caused widespread damage to property and loss of life in South Africa. On average, approximately six cyclones develop in this region per year, representing 10 percent of the yearly global total (Poolman and Terblanche, 1984). During the summer season of 1983/84 ten cyclones were reported, of which Cyclone Demoina was the largest, causing particularly severe damage over Mozambique and the eastern parts of South Africa. The development of Demoina was first observed on 17 January 1984 to the northeast of Mauritius, moving in a southwesterly direction (Fig. 4.1). By 22 January Demoina had reached the east coast of Madagascar and made landfall in the vicinity of Toamasina (Poolman and Terblanche, 1984). From here Demoina moved westward over the northern reaches of Madagascar bringing heavy rainfall to the region, moving southward into the Mozambique Channel by 24 January. Just north of the island of Europa its path changed again and the cyclone began moving in a westerly direction. Station data from the island showed that a rainfall maximum was reached approximately 3 hours before the lowest pressure of 981.5mb was recorded (Poolman and Terblanche, 1984). By the 27 January, the cyclone had moved to a position near the Mozambique coast.

The interior of South Africa was largely unaffected by the cyclone until 29 January 1984. The dominant circulation over the Guateng and Mpumalanga regions promoted clear cloud-free conditions even with a steady decrease in atmospheric pressure. On this day Demoina moved westwards and by 12h00 GMT, was situated just south of Skukuza (Poolman and Terblanche, 1984). The atmospheric pressure continued to drop steadily until about 18h00 GMT when Skukuza measured its lowest pressure of 996,3 hPa (Poolman and Terblanche, 1984). Heavy precipitation followed in the wake of the cyclone with large-scale flood damage in southern Mozambique, and the southern reaches of the South African lowveld (Fig. 4.2). The Mahamba border post between South Africa and Mozambique received in excess of 631mm between 29and 30 January (Poolman and Terblanche, 1984). By 31 January Demoina was centred over northern Natal and the resultant precipitation produced the worst flood damage in 20 years (Fig. 4.1). The Crocodile and Komati rivers over-flowed and many

bridges and roads were washed away. Although the intensity of the cyclone had diminished by the time it passed over the Natal region, significant damage and loss of life were recorded. The economic impacts to this region were severe with more than 420 000 tonnes of sugar cane destroyed, amounting to a loss of approximately R150 million (Poolman and Terblanche, 1984).

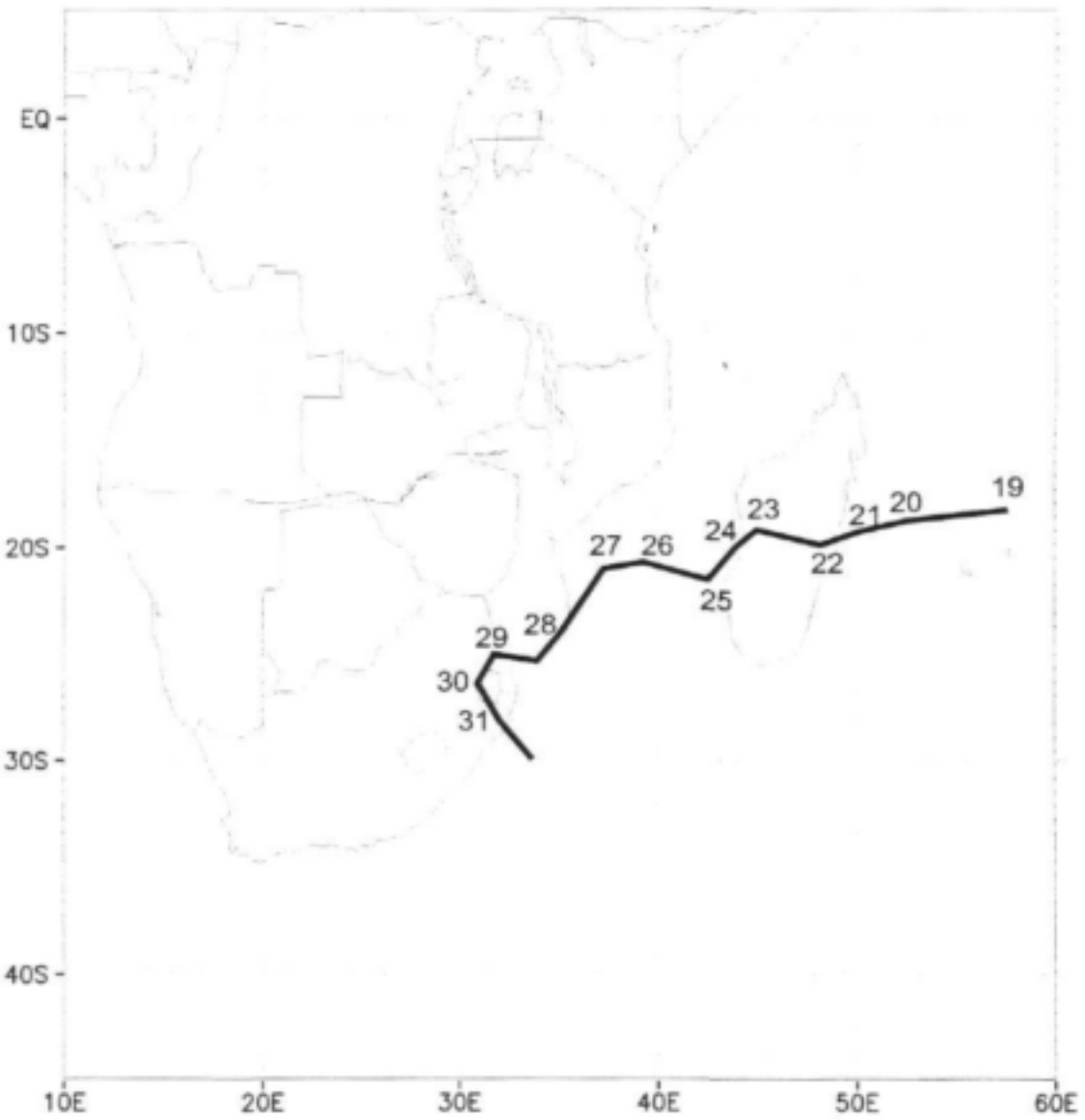

Figure 4.1: Location of the vortex of tropical cyclone Demoina plotted at 12h00 daily for the period 19-31 January 1984(after Poolman and Terblanche 1984).

Figure 4.2: South African rainfall figures for the period 28 January to 1 February 1984 (in mm, after Poolman and Terblanche 1984).

In undertaking a trajectory analysis of tropical cyclone Demoina, the aim is to improve the existing understanding of the sources of moisture and associated transport of moisture into such severe storms. The origins of moisture for this particular event have, until now remained unclear. Ten-day backward Lagrangian trajectories have been calculated using re-analysed observational data from the National Centers for Environmental Prediction (NCEP) for the second half of January 1984. The results are combined with analyses of streamflow, 500 hPa geopotential heights, precipitable water and divergence fields during selected periods to understand the development, maturation and dissipation of the cyclone as it moved southward over the southern African region.

4.2. DATA AND METHODOLOGY

The case study extends from 18 to 31 January 1984 and includes the development and dissipation of tropical cyclone Demoina. Vapour transport during this period was modelled using a backward Lagrangian trajectory methodology, whereby air parcels are advected in space and time, based on a subset of explicitly integrated equations. A more comprehensive description of the model and trajectory methodology can be found in D'Abreton (1996) and D'Abreton and Tyson (1996).

Atmospheric data was acquired from the NCEP/NCAR 40 year re-analysis project (Kalnay, *et al.*, 1996). Horizontal data resolution is limited to a 2.5° by 2.5° grid, with a vertical extent from 1000 hPa to 10 hPa. Three-dimensional wind components are used as input for the trajectory analysis. A number of atmospheric parameters were calculated from observed components of the NCEP/NCAR re-analysis data set, including streamline and divergence field values, derived from $-u$, $-v$, and $-w$ wind components. Observed atmospheric components analysed consisted of mean sea level pressure, 500hPa geopotential heights, and precipitable water were obtained from the NCEP reanlysis dataset. The record length for the atmospheric parameter analysis was somewhat longer than that of the trajectory analysis, extending from 17 January 1984 to 3 February 1984. This extended window assists in determining the pattern of

development and dissipation during the life span of Cyclone Demoina. The 500hPa geopotential height fields provide an accurate depiction of the position and vertical extent of particular synoptic features.

For this particular case study backward trajectories were performed from a designated latitude/longitude grid. The grid contains the full northeastern and southwestern extent of the cyclone's plotted track (Fig. 4.1), and in a particular case the cyclone passed directly over a release point. For analysis purposes trajectories were plotted from a number of release points and from specific vertical pressure levels, ranging from the 1000 hPa to 300 hPa. The backward trajectories plot air mass pathways backwards in time, away from the point of origin (release). This particular method of analysis provides an accurate indication of transport over time, into the point of release. The parcel's vertical ascent and decent is plotted at each time step illustrating the vertical position of the trajectory at a specific point in time.

4.3. RESULTS

Backward trajectories have been calculated for each day of the thirteen-day period from 19 January to 31 January. In each case, a cluster of 5 trajectories spaced 1° apart around a central location have been used. In general, little scatter is observed among the 5 trajectories, and therefore only the trajectory originating from the centroid is presented. The height (in hPa) at 00:00 GMT is indicated along each trajectory path. The analysis presented below is devided so as to represents key stages in the development, maturation and dissipation of tropical cyclone Demoina. For this reason, most results focus on three stages: 22 January, 1984, when Demoina was located over the east coast of Madagascar, 25 January, when it was located in the southern Mozambique Channel, and 28 January, after the storm had made landfall over Mozambique and had begun to recurve south-eastwards and dissipate.

4.3.1. East of Madagascar

On 22 January 1984, 1000 hPa streamlines indicate the location of tropical cyclone Demoina over eastern Madagascar (Fig. 4.3a). Highest precipitable water content values (in excess of 50 mm) are located to the east and north-east of the Madagascan coast (Fig. 4.3c), and the location of the storm is associated with strong convergence near the surface over the Mozambique Channel and central Madagascar (925 hPa, Fig. 4.3d) and a weak depression in 500 hPa geopotential heights to the north east (Fig. 4.3b).

Trajectories originated on 22 January 1984 from 20°S 50°E, on the east coast of Madagascar indicate the influence of the cyclonic vortex on the atmospheric circulation over the preceding days (Fig 4.4). Backward trajectories originating at 1000 hPa (Fig. 4.4a) indicate that flow is restricted below 950 hPa transport occurs around a tropical depression between 17 and 20 January. Other members of the 5-cluster trajectory display very tight recirculation near 15°S, 60°E between 19 and 20 January, indicating the location of the storm on those days (not shown). A similar trajectory pattern appears at 700 hPa (Fig. 4.4b), although significant uplift from 850 to 700 hPa and a rapid distortion of the flow pattern is indicated between 19 and 22 January as the storm approaches Madagascar. Backward trajectories from 500 hPa (Fig 4.4c) on 22 January originate near the surface at approximately 5°S and 50°E ten days earlier. Trajectories follow a gradually rising path as they are transport initially eastward and then recurved east of 70°E on the 16th. The location of the cyclone vortex is indicated clearly by the recurved flow on the 19th, 20th and 21st, during which time the parcel is lifted from approximately 700 hPa to 500 hPa. A similarly tight vortex is indicated by the 300 hPa trajectory (Fig. 4.4d), which indicates a more constant easterly inflow from the surface near 10°S 80°E.

Note that while most backward trajectories originate indicate a flow pattern originating near the surface at the equator, east of 50°E. The most significant uptake of moisture, however, is likely to occur on the days immediately preceding 22 January, as the transport occurs through the region of high precipitable water content (Fig. 4.3c).

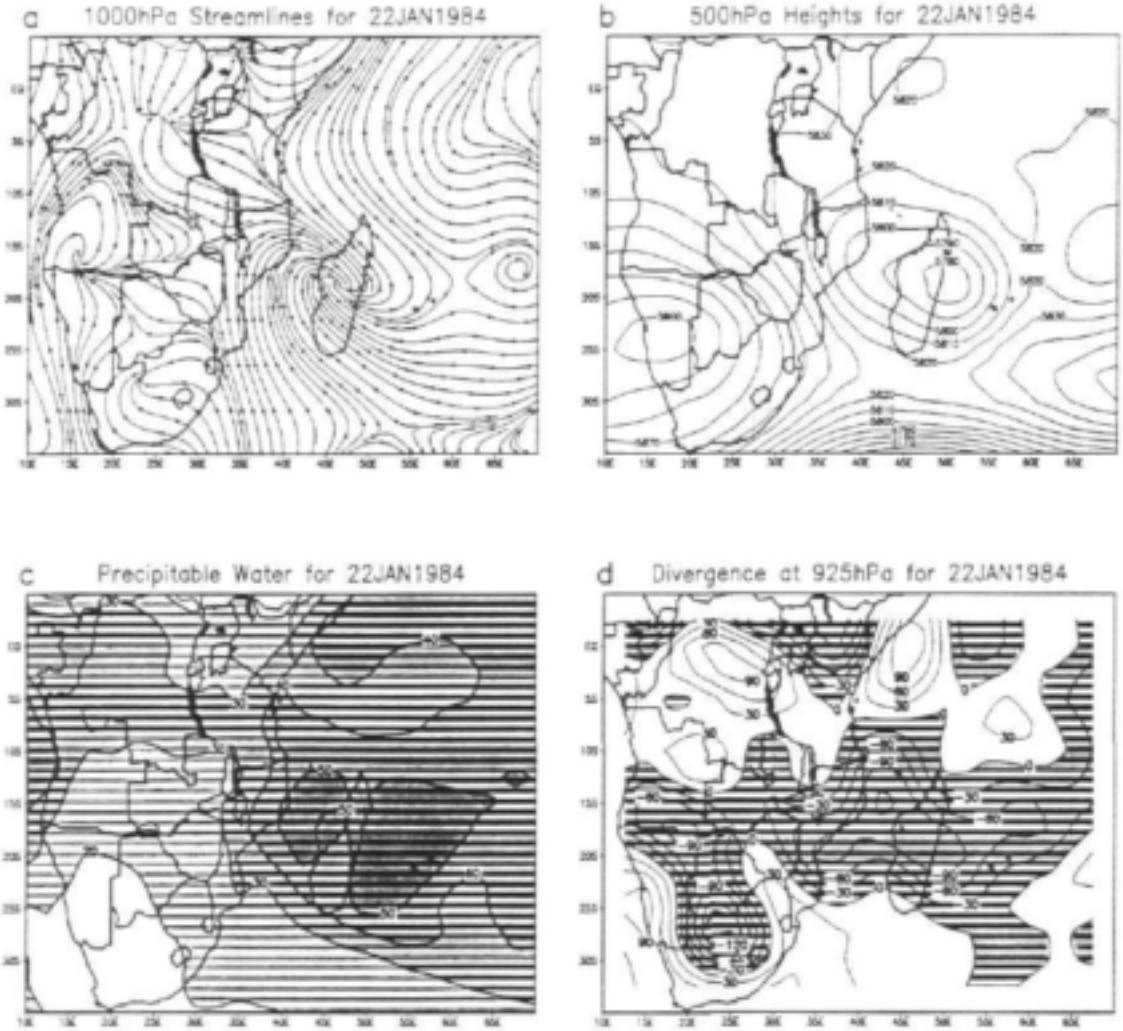

Figure 4.3: (a) 1000 hPa streamlines, (b) 500 hPa geopotential heights, (c) precipitable water (mm) and (d) 925 hPa divergence fields [??units] for 22 January 1984.

4.3.2. Mozambique Channel

Streamlines at 1000 hPa for 25 January indicate the location of Demoina over the southern Mozambique Channel (Fig. 4.5a). The depression in 500 hPa geopotential heights is more strongly developed (Fig 4.5b) and is located directly overhead a region of strong surface (925 hPa) convergence (Fig 4.5d), and maximum precipitable water contents (Fig. 4.5c).

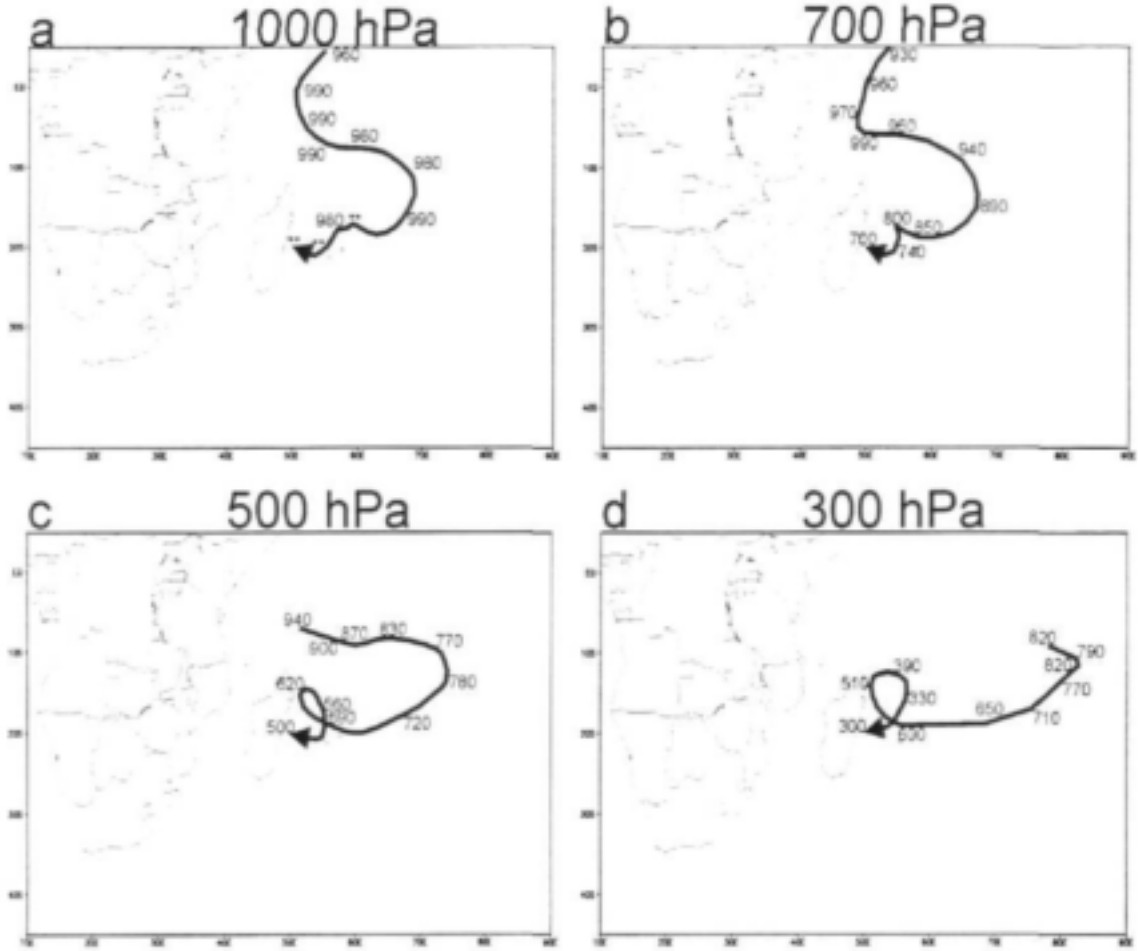

Figure 4.4: Backward trajectories starting on 22 January 1984 at 20°S 50°E, for the (a) 1000 hPa, (b) 700 hPa, (c) 500 hPa and (d) 300 hPa levels. Heights (in hPa) are indicate along the trajectory path at 00h00 GMT every day. Heights below 1000 hPa are indicated by a double-asterisk (**).

Backward trajectories starting on 25 January from 1000 hPa at 20°S 40°E indicate an inflow of colder, drier air from the south and west which originates in the South Atlantic near 30°E (Fig. 4.6a). The 700 hPa trajectories indicate a de-coupled airflow from the east which rises slowly as it travels westward (Fig. 4.6b). The major uplift and tight vortex associated with the cyclone itself is clearly indicated from the trajectories which reach 500 hPa on the 25th (Fig. 4.6c). These trajectories originate only slight further north of 20°S on the Mozambique coast and flow west across Madagascar before being recurved near 50°E on the 22nd. As the trajectories pass

through the wall of the storm, they are lifted dramatically from the surface to the 500 hPa level. The origin of the 500 hPa trajectories is coincident with the region of maximum precipitable water shown in Figure 4.5c. Trajectories arriving at 300 hPa on the 25th originated near the equator at 50°E, and also display rapid uplift as they reach the Madagascan coast and the wall of the storm (Fig. 4.6d).

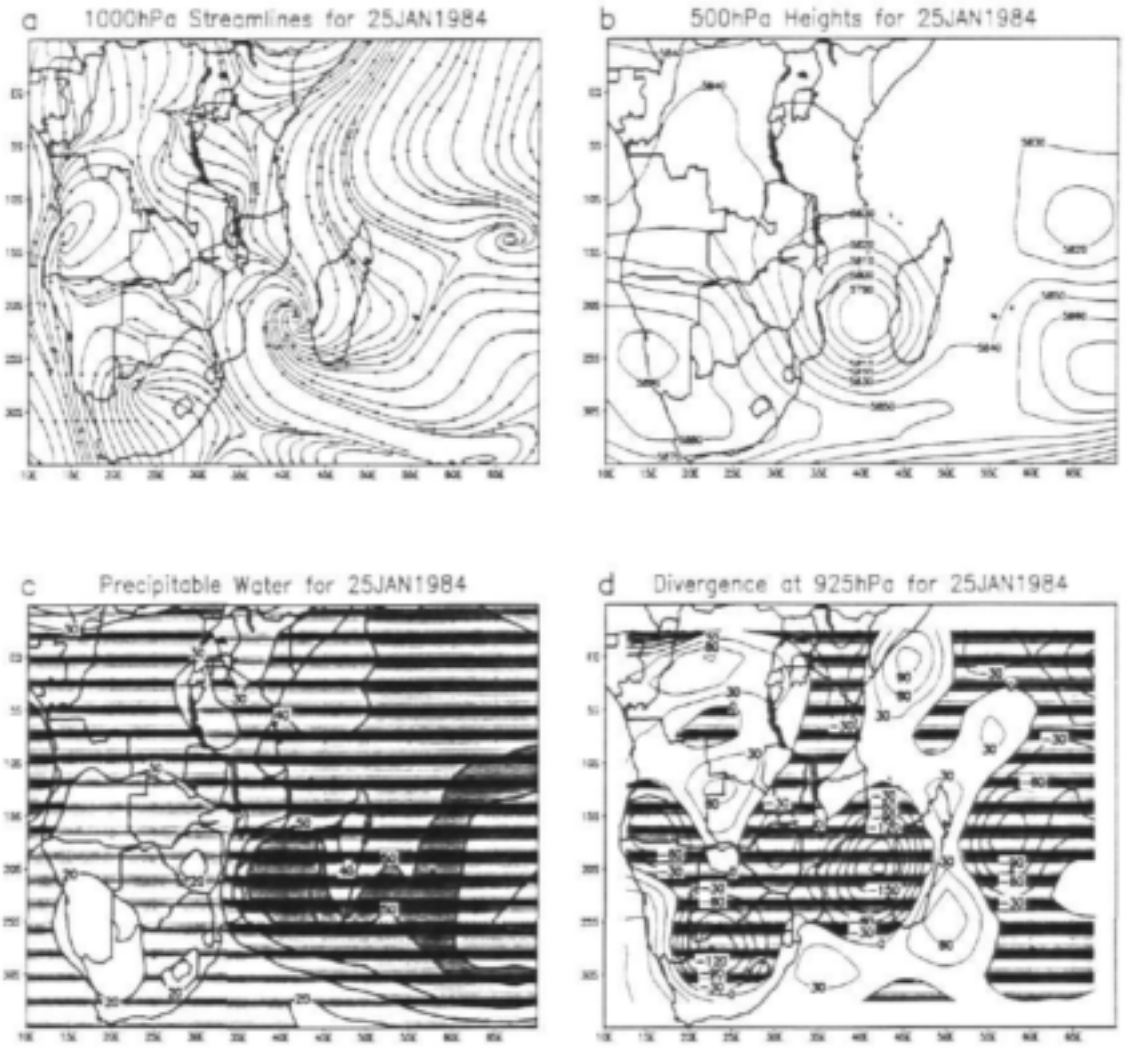

Figure 4.5: As for Figure 4.3 but for 25 January 1984.

4.3.3. Landfall over Mozambique

Demoina made landfall over Mozambique on 28 January (Fig 4.7a). The westward shift in the location of the storm is reflected at 5000 hPa (Fig. 4.7b) and in the

precipitable water contents (Fig. 4.7c). Precipitable water contents over the location of the storm remain in excess of 50 mm, although higher precipitable water content is located the the south and east of the location of the cyclone. With its landfall, the system as begun to be separated from its moisture source over the Mozambique current, and as a result, convergence at 925 hPa has weakened (Fig. 4.7d).

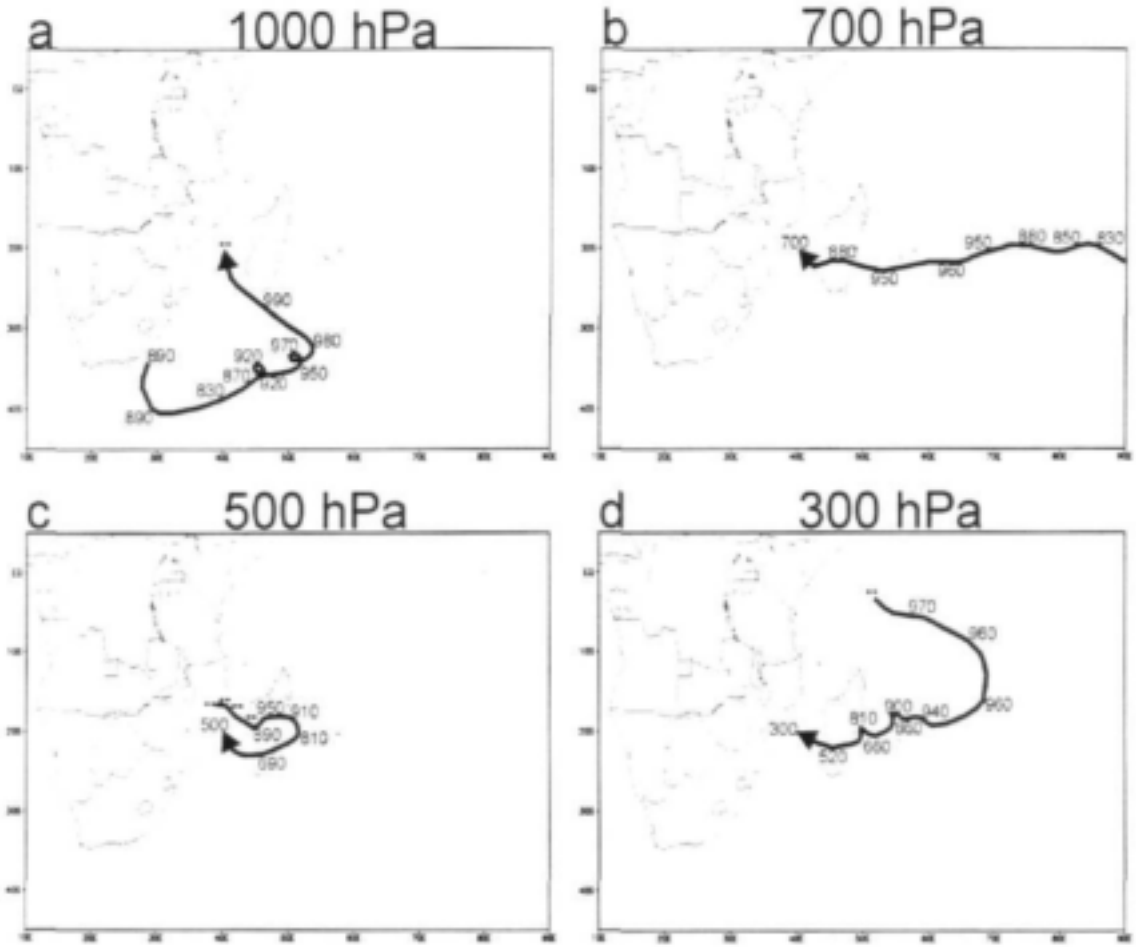

Figure 4.6: As for Figure 4.4 but for a starting point at 20°S 40°E and backward trajectories starting on 25 January 1984.

Backward trajectories which reach 1000 hPa at 20°S 40°E indicate the cyclonic curvature over central Mozambique (Fig. 4.8a). These trajectories originate in the South Atlantic Ocean near 800 hPa, and indicate a gradual inflow of a colder, drier air mass (Fig. 4.8a). The descending nature of this air mass is more clearly indicated at the 700 hPa level, with trajectories reaching the 450 hPa on 22 January south of Port Elizabeth (Fig 4.8b). The dissipation in the intensity of the tropical cyclone is

indicated by the relatively gradual uplift from 770 hPa to 700 hPa as the trajectories pass over the location of the storm. Trajectories arriving at 500 hPa on the 28th originated in the central south Indian ocean, and are descending as they are affected by the vortex over Mozambique (Fig. 4.8c). At 300 hPa, the trajectories indicate and extensive anticyclone curvature, with gradual descent from 200 hPa to 300 hPa (Fig. 4.8d).

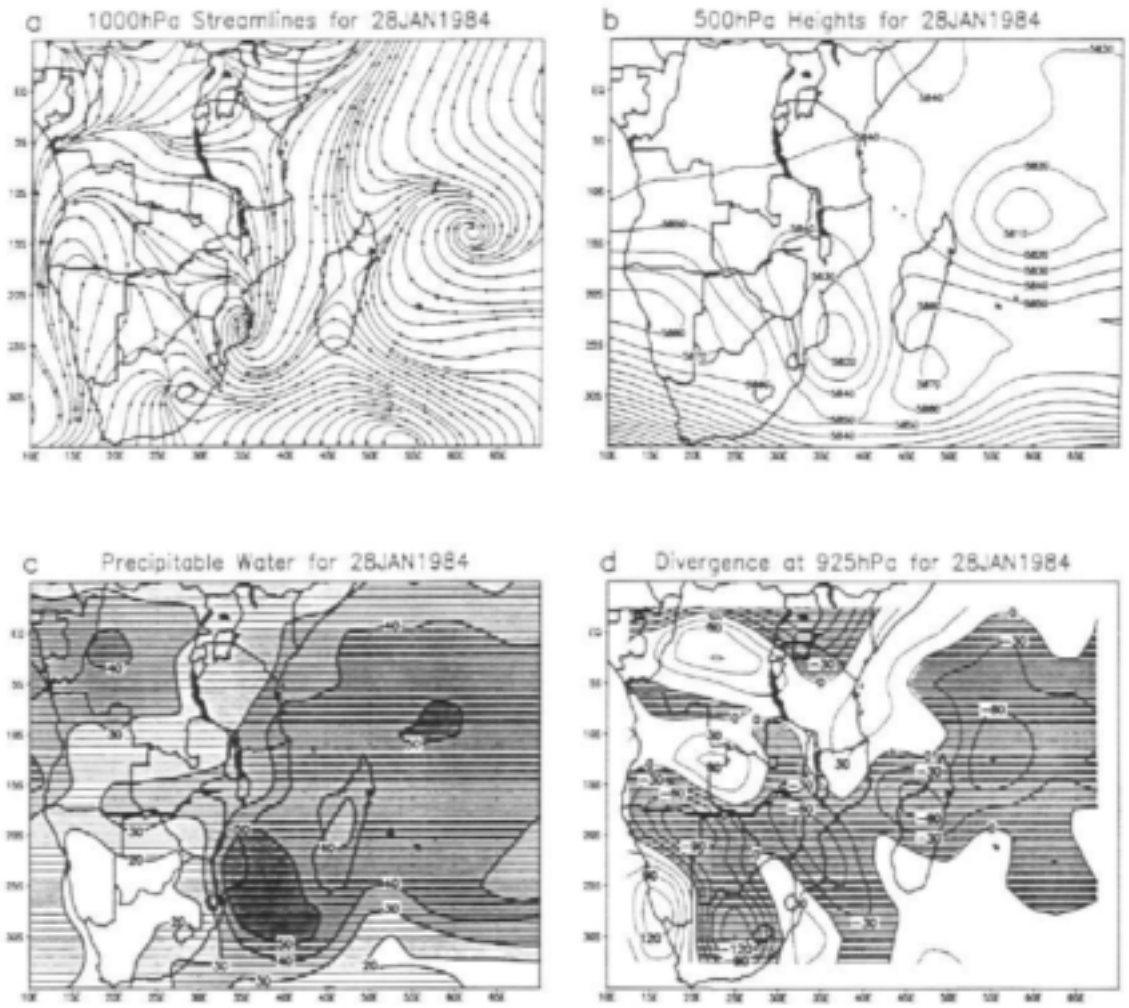

Figure 4.7: As for Figure 4.3 but for 28 January 1984.

4.4. DISCUSSION AND CONCLUSIONS

Backward trajectories for the second half of January 1984 have been used to identify the moisture sources and airflow associated with tropical cyclone Demoina. A summary of all trajectories calculated is presented in Figures 4.9 and 4.10. The total

number of trajectories which strike a series of meridional and zonal "walls" located 10° apart has been calculated. These are presented as percentages of the total number of trajectories which strike a meridionally-oriented wall from the west or east (representing westerly and easterly transport, Fig. 4.9), or a zonally-oriented from the north or south (northerly or southerly transport, Fig. 4.10). The central location for both diagrams is located in the southern Mozambique Channel at 20°S 40°E.

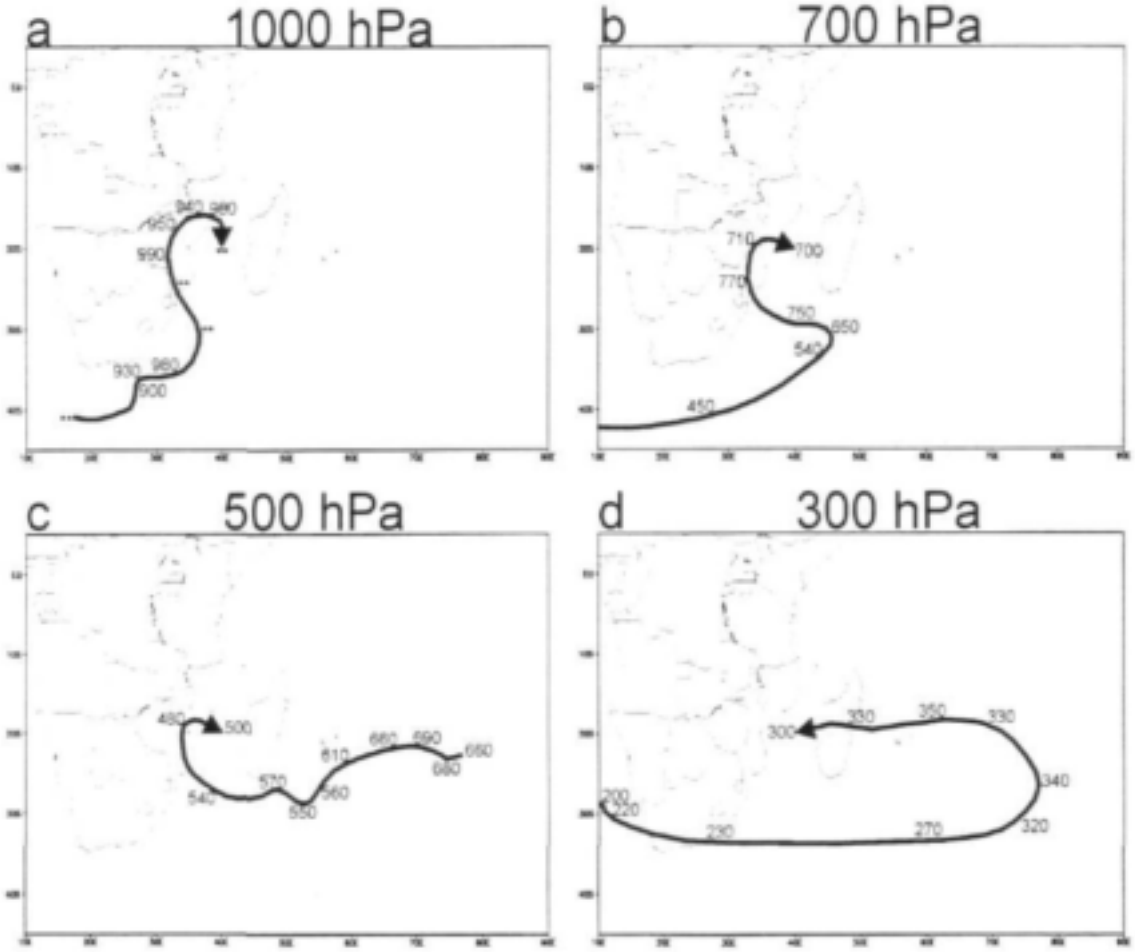

Figure 4.8: As for Figure 4.4 but for backward trajectories starting on 28 January 1984.

For zonal transport, more than twenty percent of all trajectories are transported from the east between 20°S and 30°S (Fig. 4.9b). There is another important inflow of air from the southern Atlantic Ocean, represented a westerly airflow (Fig. 4.9a). Westerly airflow reaches it's maximum in the immediate vicinity of 20°S 40°E, indicating the tight vortex and cyclonic curvature of the tropical cyclone itself. For meridional

transport, in excess of 50 percent of all trajectories which strike zonally-oriented walls from the south are associated with the immediate location of the storm, and again indicate the tightly recirculating flow associated with the cyclone vortex (Fig. 4.10a). Northerly flow occurs from two origins; a region east and north-east of Madagascar, and a region extending north of the equator along the east African coast.

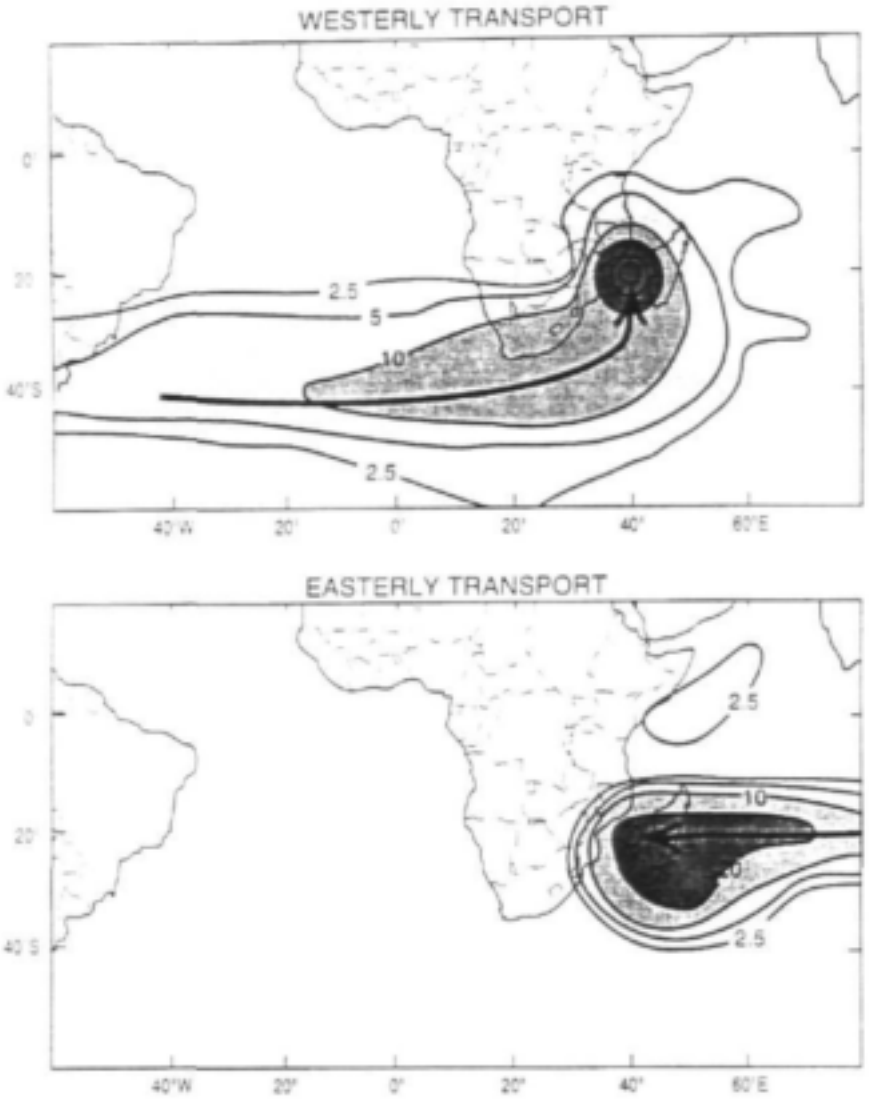

Figure 4.9: Percentage of all backward trajectories originating at 20°S 40°E which strike meridionally-oriented walls located at 10° of longitude apart from either (a) westerly or (b) easterly direction.

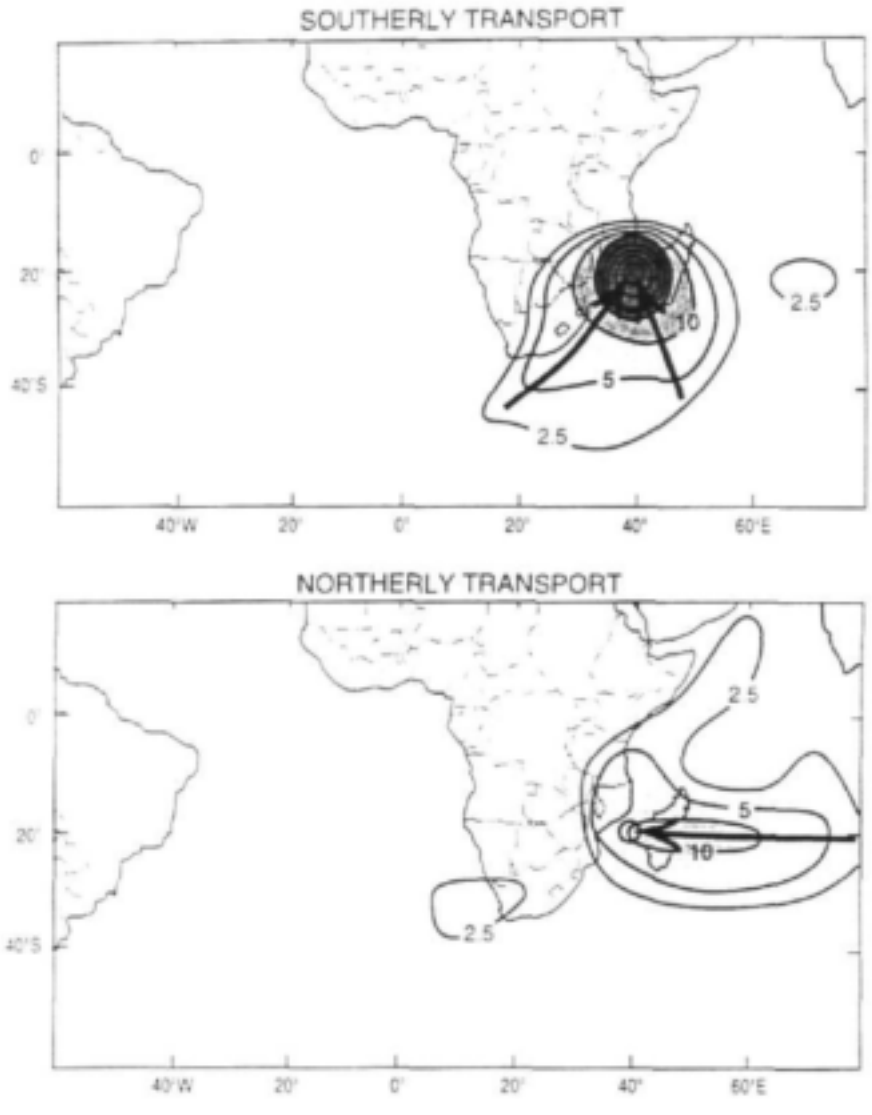

Figure 4.10: Percentage of all backward trajectories originating at 20°S 40°E which strike zonally-oriented walls located at 10° of longitude apart from either (a) southerly or (b) northerly direction.

Considered in conjunction with the individual trajectories, and locations of moisture and convergence, several conclusions can be drawn. Firstly, the primary source of moisture for tropical cyclone Demoina was highly localised and associated with the vortex itself. Backward trajectories indicate an inflow from the east into the system from the central tropical Indian Ocean, associated with very rapid uplift of moisture from the surface within the walls of the cyclone itself. A secondary airflow pattern

from the South Atlantic region introduces colder, drier air from the south-west, which is generally descending as it reaches the location of the cyclone vortex. It is hypothesised that this inflow provides a wedge of more stable, colder air against which the uplift in the cyclone can occur, and is similar in principle to the model described by D'Abreton and Tyson (1996) in their investigation of the atmospheric circulation associated with the Laingsburg floods of January 1981.

Kinematic trajectory analysis has proved a useful tool in attempting to understand the structure of tropical cyclone Demoina. The approach has demonstrated that the majority of moisture available to the system is transported over very short distances within a tight vortex, and uplifted rapidly to approximately 500 hPa within the storm. A secondary airflow of colder, drier airflow, originating from the south-west is an important component of the system, however, as it supplies a "wedge" of colder, subsiding air against which the tropical cyclone can advance.

CHAPTER 5

DAILY RAINFALL SIMULATIONS OVER SOUTH AFRICA USING A NESTED REGIONAL CLIMATE MODEL[1]

5.1. INTRODUCTION

General circulation models (GCMs) provide increasingly realistic simulations of present and future global climates, but do not yet resolve the small-scale circulation features important for accurate simulations of regional climate. Limited area models (LAMs) nested within global climate models or observational analyses, are capable of representing the detailed features of orography and land surface which affect regional climate (McGregor, 1997). More recently known as regional climate models (RCMs), nested models have been used to provide regional climate simulations for several regions, including the United States, Europe, Australia, New Zealand, South-East Asia and South America. Reviews of previous regional modelling studies and approaches have been provided by Giorgi and Mearns (1991), Giorgi (1995) and McGregor (1997).

Most existing regional climate model experiments have been performed as multiple month-long (usually January and July) simulations, nested within observational analyses (Giorgi and Marinucci, 1991; Giorgi et al., 1993a,b; Walsh and McGregor, 1996) and within GCM simulations under idealised present-day (1 x CO_2) conditions (Giorgi, 1990; Marinucci and Giorgi, 1992; McGregor and Walsh, 1993, 1994; Marinucci et al., 1995; Walsh and McGregor, 1995). These simulations have

---

[1] These results were presented at the "Conference on the Role of Topography in Modelling Regional Weather and Climate", International Centre for Theoretical Physics, Trieste, Italy, 22-26 June 1998. The paper was co-authored by Drs J.J. Katzfey and J.L. McGgregor (CSIRO Atmospheric Research, Melbournce, Australia).

demonstrated that RCMs are generally able to simulate the details of regional climate better than the GCM, although rainfall is often over-estimated in regions of steep orography (e.g. Giorgi et al., 1994; Giorgi et al., 1995). Seasonally varying present-day and future climate (2 x CO_2) simulations for the United States, Europe and Australasia have also been completed using nested modelling techniques (Giorgi et al., 1993a,b; Giorgi et al., 1994; Giorgi and Marinucci, 1996; Walsh and McGregor, 1997; Renwick et al., 1998).

Over southern Africa, several evaluations of the regional performance of global models, and estimates of possible future climate based on GCMs are available (Joubert, 1994, 1995, 1997; Joubert and Tyson, 1996; Hudson, 1997). To date, very few attempts have been made to simulate regional climate over Africa using a nested modelling approach. Sun et al. (1997) used the NCAR MM4 RegCM2 model (Giorgi et al., 1993a,b) to perform sensitivity studies for a seasonal climate prediction scheme over tropical east Africa. They demonstrated the sensitivity of the RegCM2 model to several physical parameterisations, including those for convection, moisture, boundary layer configuration, surface physics and lateral boundary schemes.

Simulations of regional climate from GCMs, particularly in the case of rainfall, are unreliable due to the coarse resolution of such models, and there is a clear need to provide accurate simulations of present and future climate which account for regionally specific climate forcings and processes (Joubert and Hewitson, 1997). Nested regional modelling approaches are well suited to this objective (e.g. *Giorgi*, 1995). In this study, results are presented from the Commonwealth Scientific and Industrial Research Organisation (CSIRO) Division of Atmospheric Research limited area model (DARLAM), nested within the CSIRO9 Mark 2 GCM (Watterson et al., 1995) over the southern African region. The ability of the regional model to simulate daily rainfall during January (the peak rainfall month over southern Africa) is assessed. While gridded rainfall observations are used, all other observations are based on National Centres for Environmental Prediction (NCEP) reanalyses (Kalnay et al., 1996). An earlier assessment of the performance of the nested model (simulating only Januaries) has been described by Joubert *et al.* (1998). In this study,

we assess a seasonally-varying simulation and concentrate specifically on daily rainfall statistics.

5.2. THE NESTED MODEL AND EXPERIMENTAL DESIGN

DARLAM is nested within the CSIRO9 atmospheric GCM, which is a spectral model run at R21 resolution with nine sigma vertical co-ordinate levels (Watterson et al., 1995). Using the flux form of the dynamical equations, the GCM achieves conservation of mass and global energy, which makes it suitable for use for climate simulation. For these simulations, the CSIRO9 model used a mixed-layer ocean with "Q-fluxes" to calculate the sea-surface temperatures (for more details see Watterson et al., 1995). Ocean heat fluxes calculated in this way do not accurately represent observed ocean heat transport, nor do they respond to inter-annual variations of the surface conditions. So for example, inter-annual variability related to El Niño / Southern Oscillation (ENSO) events is not represented in either the CSIRO9 or DARLAM climatologies.

DARLAM is a two-time-level, semi-implicit, hydrostatic primitive equations model, developed for both mesoscale studies and climate change experiments. The model uses an Arakawa staggered C-grid and semi-Lagrangian horizontal advection with bicubic spatial interpolation (McGregor, 1987; Walsh and McGregor, 1995). DARLAM uses the same 9-level vertical structure as the CSIRO9 GCM and incorporates a comprehensive set of physical parameterisations. The cumulus convection scheme adopted for these experiments is a modified version of the Arakawa (1972) "soft" moist adjustment cumulus convection scheme and uses a mass flux closure. Several other convection schemes have been tested in earlier (unpublished) sensitivity tests. The precipitation scheme adopted here performed better over numerous multiple single-month sensitivity tests. The convection scheme allows for evaporation of both large-scale (resolved) and convective (parameterised) rainfall. The model also includes enhanced surface drag near mountainous terrain to account for subgrid-scale orographic drag. Further details of these parameterisations

and of the vertical mixing scheme are provided by McGregor et al. (1993). Vegetation data, including soil and vegetation type, physical characteristics associated with these, and albedo were derived from the Simple Biosphere Model (SiB) data (Dorman and Sellers, 1989). These are utilised by the surface canopy scheme of Kowalczyk et al. (1994). The US Navy 5' orography is aggregated to the model's 125-km resolution Lambert conformal grid.

A one-way nesting strategy is adopted here, with lateral boundary conditions and sea-surface temperatures for the regional climate model specified by the CSIRO9 Mark 2 GCM (Watterson et al., 1995). At each time step, the outermost DARLAM boundary rows are relaxed toward the interpolated values provided every 8 hours by the GCM, using the nesting procedure of Davies (1976), but with exponentially-decreasing weights. Initial conditions for DARLAM including soil moistures, are provided by the forcing GCM. Sea-surface temperatures are provided every 8 hours by the GCM. In this experiment (unlike that discussed by Joubert *et al.*, 1998), the full seasonal cycle is represented by the model, in a 10-year simulation using present-day atmospheric CO_2 concentrations.

The southern African region, its political boundaries and model representations of its orography are shown in Figure 5.1. The interior of southern Africa is characterised by an elevated plateau with altitudes in excess of 1000 m (Fig. 5.1b). Maximum altitudes in excess of 3500 m occur along the South African escarpment, as well as over equatorial east Africa. The coastal margins along the east and southeast coast of southern Africa are narrow and marked by steep orographic gradients. The R21 spectral resolution of the CSIRO9 GCM results in a very smoothed representation of orographic features over southern Africa. The plateau is narrow, maximum altitudes are under-estimated by as much as 2500 km, and orographic gradients along the edge of the escarpment are relatively gentle (Fig. 5.1b). With a horizontal resolution of 125 km, DARLAM provides a more realistic representation of regional topographic features over southern Africa than the GCM (Fig. 5.1c). Highest elevation in DARLAM (in excess of 1800 m above sea level) is reached over the escarpment of Southeast South Africa. Features such as the South African escarpment are much more clearly resolved at the 125-km resolution than they are by the GCM.

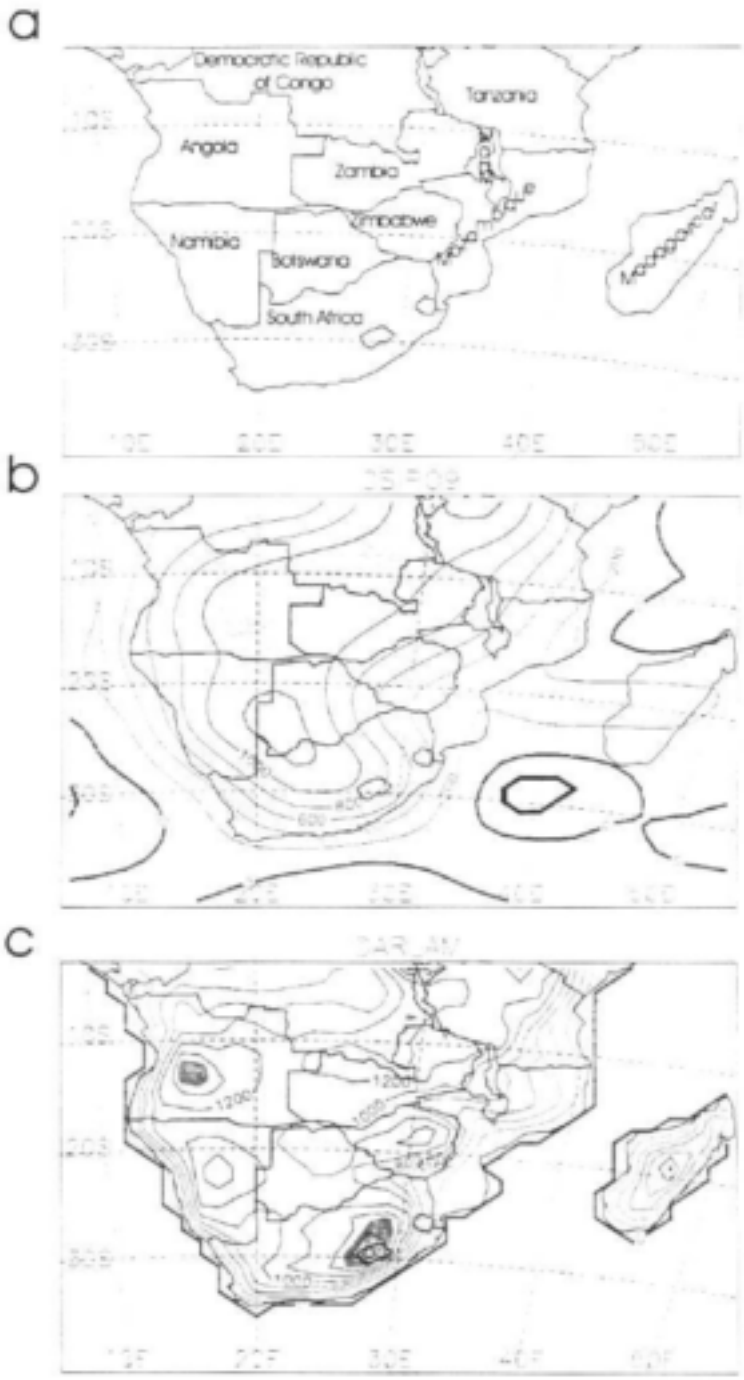

Figure 5.1. Political boundaries (a) and orography of the southern African region for (b) the CSIRO9 GCM and (c) DARLAM 125 km grid. Contour interval is 200 m. Elevations above sea-level are shaded between 500 m and 1000 m (light grey), 1000 m and 1500 m (grey) and above 1500 m (dark grey).

5.3. VALIDATION DATA

Observed mean sea-level pressures, u- and v-wind components, temperatures and mixing ratios are taken from the NCEP reanalysis data (Kalnay et al., 1996). Means for the period 1982-1994 at 2.5° x 2.5° resolution and 17 vertical levels have been interpolated to the DARLAM grid using a 16-point bicubic Bessel interpolation procedure (also adopted for interpolating the GCM data to DARLAM resolution).

The period over which the NCEP reanalysis averages are calculated includes three ENSO-related summer drought periods over southern Africa (1982-3, 1987 and 1991-2). Being a slab-ocean model using a prescribed q-flux procedure calculated using climatological sea-surface temperatures, the CSIRO9 Mark 2 simulation does not incorporate ENSO variability.

For land precipitation data, daily gridded data, at 0.5° resolution, were obtained from the Department of Agricultural Engineering, University of Natal, Pietermaritzburg. These data extend over the period 1950-1994. Ten-year periods for 1950-59, 1960-69, 1970-79 and 1980-89 have been averaged for comparision with the ten-year regional model statistics.

5.4. RESULTS

5.4.1. Mean January Climate

5.4.1.1. Daily rainfall

Simulated and observed rainfall statistics, indicating average daily rainfall, the average number of rain days and rain per rain day (rainfall intensity) are shown in Figure 5.2. DARLAM simulates the marked east-west gradient in January rainfall (Fig. 5.2a) over south Africa well, although daily rainfall magnitudes are over-estimates in all regions east of 25°E. The over-estimate of daily rainfall totals is most

serious in the vicinity of the escarpment over Kwazulu/Natal, extending northwards into Mpumalanga. In this region, DARLAM simulates as much as three times as much daily rainfall as is observed (Fig. 5.2a, b).

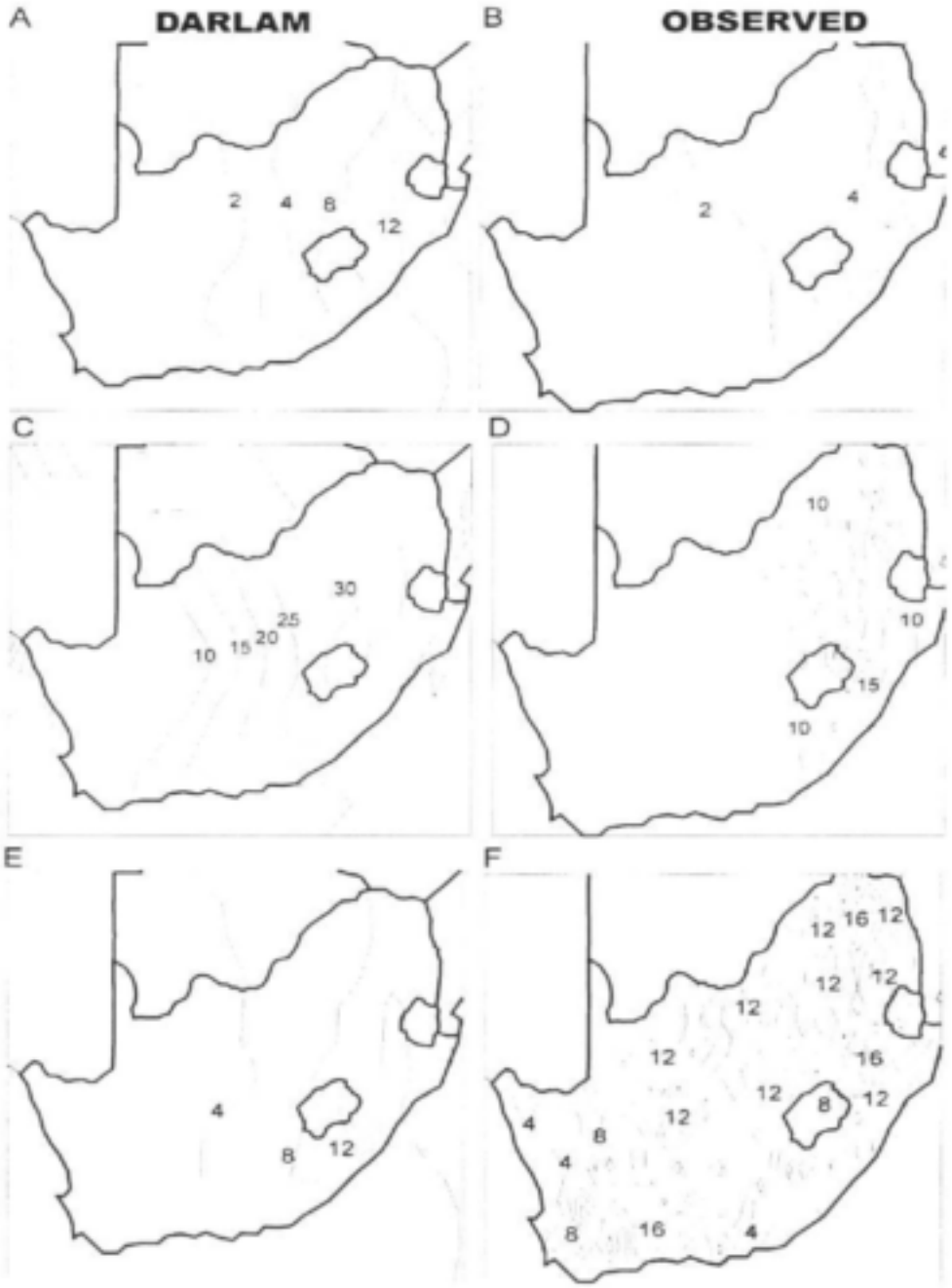

Figure 5.2. Average daily rainfall (in mm) for January simulated using DARLAM (a) and observed (b); simulated (c) and observed (d) average number of rain days; and simulated (e) and observed (f) rain per rain day (rainfall intensity, in mm/day). Rain days are defined as rainfall in a 24-hour period in excess of 0.2 mm.

Observed rainfall intensities reflect local-scale topographic variability closely, with highest intensities along the steepest gradients such as the southern Cape, the escarpment region of Kwazulu/Natal and Mpumalanga, and the northern parts of Northern Province (Fig. 5.2f). By contrast, the rainfall intensities simulated by DARLAM (Fig. 5.2e) reflect a much smoother distribution, although highest intensities also occur along the steepest topographic gradients along the southeastern escarpment. In this region, simulated daily rainfall intensities are comparable to observations in magnitude.

5.4.1.2. Daily Rainfall frequency distribution

Simulated daily rainfall and numbers of rain days are most exaggerated over the Drakensberg escarpment. The simulated daily rainfall frequency distribution in this region is illustrated in Figure 5.3. Frequencies are expressed as probabilities of occurrences of rainfall events of a given magnitude, expressed as a percentage of all rainfall events (in excess of 0.2 mm/day). Rainfall classes are defined according to a logarithmic scale, in order to ensure that rainfall events are approximately normally distributed.

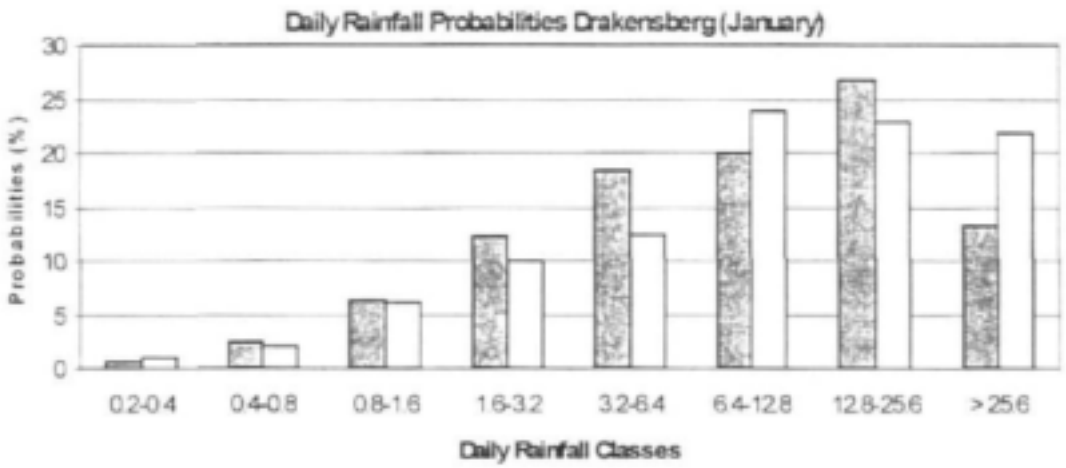

Figure 5.3. Simulated (grey) and observed (open) frequency distribution of daily rainfall for a single location (model grid box) over the Drakensberg escarpment (approximately 28.5°S, 30.5°E). Frequencies are expressed as probabilities of occurrence (frequency/total number of rain days * 100) for a logarithmically-increasing range of daily rainfall classes.

The occurrence of light rainfall events (daily rainfall < 3.2 mm/day) is well-simulated by DARLAM. The frequency of moderate rainfall events (3.2 < rainfall < 25.6 mm/day) is generally over-estimated by DARLAM, by as much as 5 per cent. Heavy rainfall events (> 25.6 mm/day) are less likely to occur in the regional model simulation than in observations. Overall, the shade of the simulated frequency distribution is largely similar to that which is observed.

5.4.1.3. Specific humidity

Simulated and observed specific humidities are shown in Figure 5.4. DARLAM captures the east-west gradient in near-surface moisture (810 hPa) across southern Africa south of 20°S well, although moisture values along the east coast (Kenya, Mozambique, northern Kwazulu/Natal) are higher than observed (Fig. 5.4a, b). Given that moisture values are highest near the surface along the east coast, a zonal profile of moisture between the surface and 500 hPa through 30°E is also presented (Fig. 5.4c, d). Note that the profile broadly follows the escarpment region of the East African Rift Valley. The Highlands region of eastern Zimbabwe, as well as the South African escarpment result in a pronounced adjustment of the zonal moisture profile north of 20°S and near 30°S. The adjustment in the profile in the observed NCEP fields is possibly slightly more pronounced than in DARLAM, and moisture values at the surface near 20° and 30°S are slightly higher than in the regional model. Overall, the simulated profile is largely similar to the observed profle, both in magnitude and shape.

5.4.1.4. Vertical velocity

During January, slow uplift occurs on average at the surface (980 hPa) over most of the southern African subcontinent, as well as south-east of the land (Fig. 5.5a). Strongest uplift occurs along the Kwazulu Natal coast, on the coastal side of the escarpment (> 0.2 hPa/s). Descending motion occurs on average over the oceans the the east, west, and south-west of the subcontinent (Fig. 5.5a).

The vertical profile of vertical velocities through 30°E (Fig. 5.5b) indicates strongest uplift near the Kwazulu/Natal escarpment, although upward motion is experienced

throughout the troposphere between the equator and 25°S. On average, air is descending south of 35°S, between the surface and approximately 500 hPa, as well as in the upper troposphere, extending downwards to 700 hPa near 30°S.

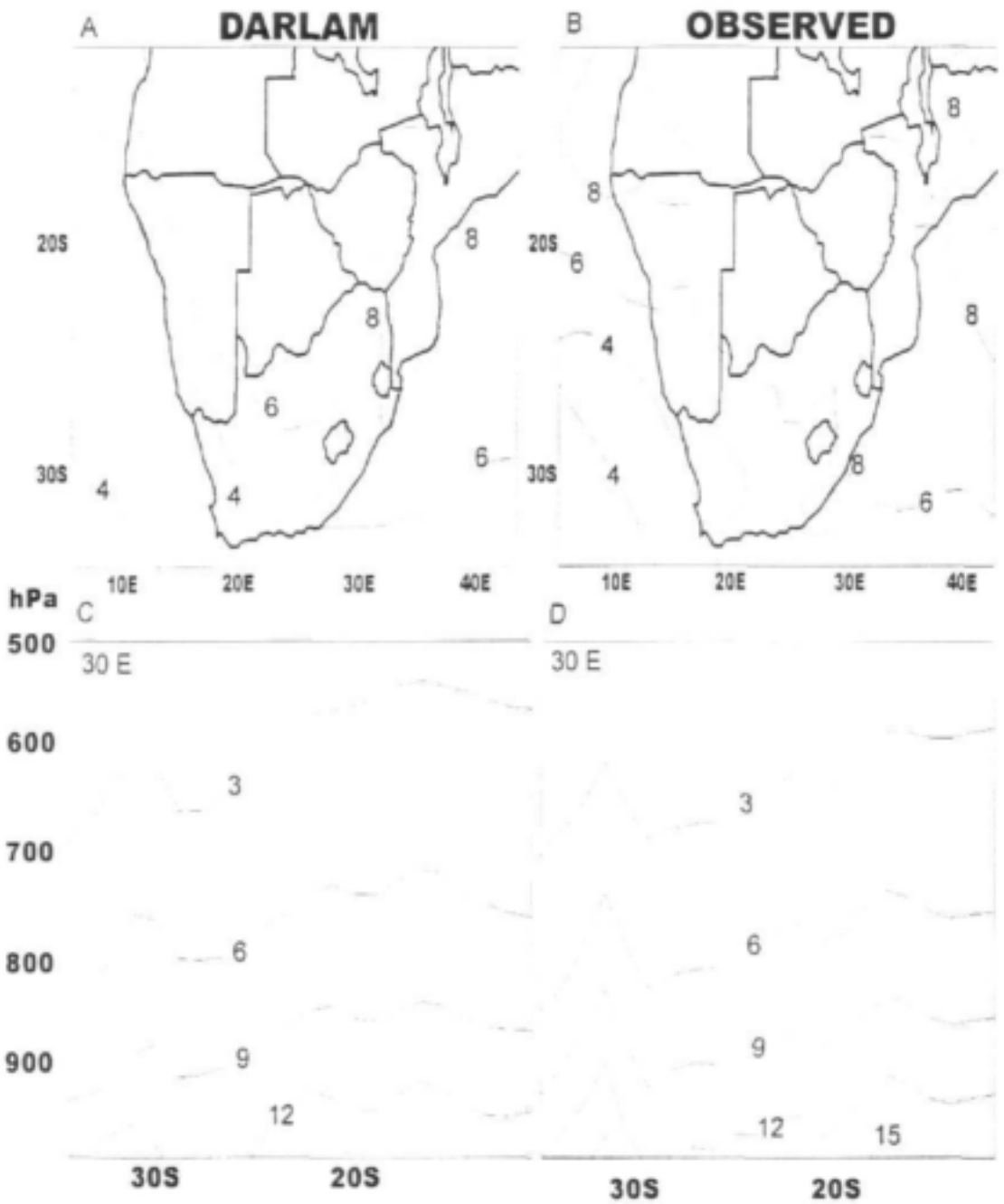

Figure 5.4. Simulated (a) and observed (b) 810 hPa specific humidities in January (g/kg), as well as simulated (c) and observed (d) zonal profiles of specific humidity (g/kg) calculated along 30°E.

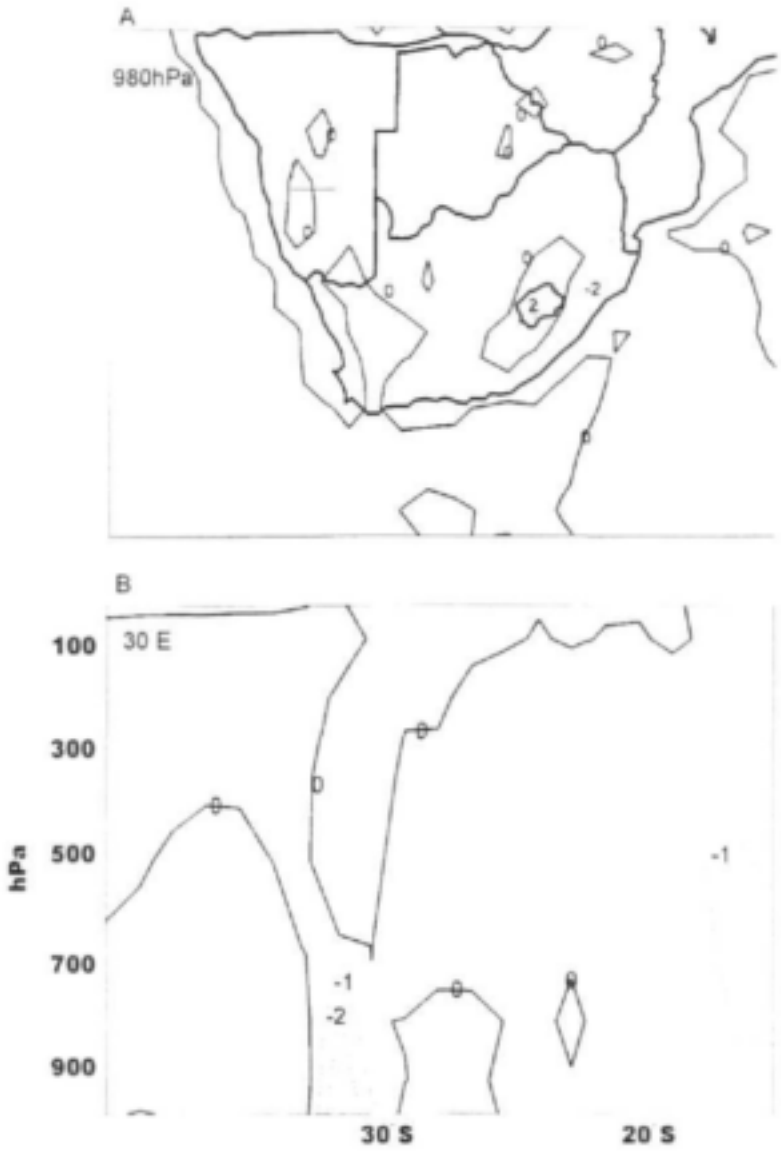

Figure 5.5. (a) Simulated vertical velocities at the surface (980 hPa); (b) vertical profile of vertical velocities through the model troposphere along 30°E (in Pa/s * 10). Negative vertical velocities (uplift) are indicated by dashed lines.

5.4.2. Circulation During Above-Normal Rainfall Events

DARLAM simulates more total rainfall and more rain days than observed, particularly over regions of steep topography such as the Kwazulu/Natal escarpment. The aim in this section is to investigate the causes of this over-estimate. In order to do this, statistics are calculated for a single model grid-point on the upslope of the model

escarpment (located at approximately 28.5°S, 30.5°E, at an altitude of approximately 1200 m). Sea-level pressure, wind, specific humidity and vertical velocity anomalies are calculated for all days over the ten consecutive Januaries used in the model simulation, for which rainfall was *above aveerage* at this grid point.

5.4.2.1. Sea-level pressure anomalies

On average, above-normal rainfall events along the escarpment of South Africa are associated with positive sea-level pressure anomalies to the south of the subcontinent in the regional model (Fig. 5.6a). This pattern indicates the persistent occurrence of anticyclonic ridging by the South Atlantic Anticyclone during above-average rainfall events. This suggests an inflow of cool, moist maritime air onshore, and represents a familiar pattern for observed heavy rainfall events (e.g. Tyson, 1986). While pressure are above-normal to the south of the subcontinent, they are above-normal over northern Mpumalanga and southern Zimbabwe, indicating a region of low-level convergence.

5.4.2.2. Wind vector anomalies

Wind vector anomalies associated with above average rainfall over the escarpment indicate that anticyclonic circulation is throughout the lower troposphere between the surface and 500 hPa (Fig. 5.6b-d). At the surface (980 hPa, Fig. 5.6b), the anomalously anticyclonic flow is centred near 40°S, 25°E, with anomalously southerly flow in excess of 2 m/s over the Kwazulu/Natal coast. The flow is therefore onshore and upslope. At 800 hPa, the anomalously anticyclonic flow is located slightly further west (indicating a westward tilt with height), with anomalous onshore flow along the south and east coast of south Africa (Fig. 5.6c). As at the lower level, there is a marked convergence zone stretching from the southern Lowveld region of Mpumalanga and northern Kwazulu/Natal, eastwards out into the South Indial Ocean, where the anomalously southerly flow encounters anomalous flow from the north and west. The pattern would indicate a south-easterly transport of moisture from a source region (probably within the tropics), with convergence occurring south-eastwards from Swaziland. At 500 hPa, the anticyclonic anomaly pattern is located further to the

west and south, with a cyclonic anomaly pattern located over the South Indian Ocean to the south east of the subcontinent (Fig. 5.6d). Flow at this level is markedly stronger than at the lower levels, with offshore anomalies on the west coast exceeding 4 m/s. At this level, convergence occurs south of East London, shifted south of the location of convection at lower levels.

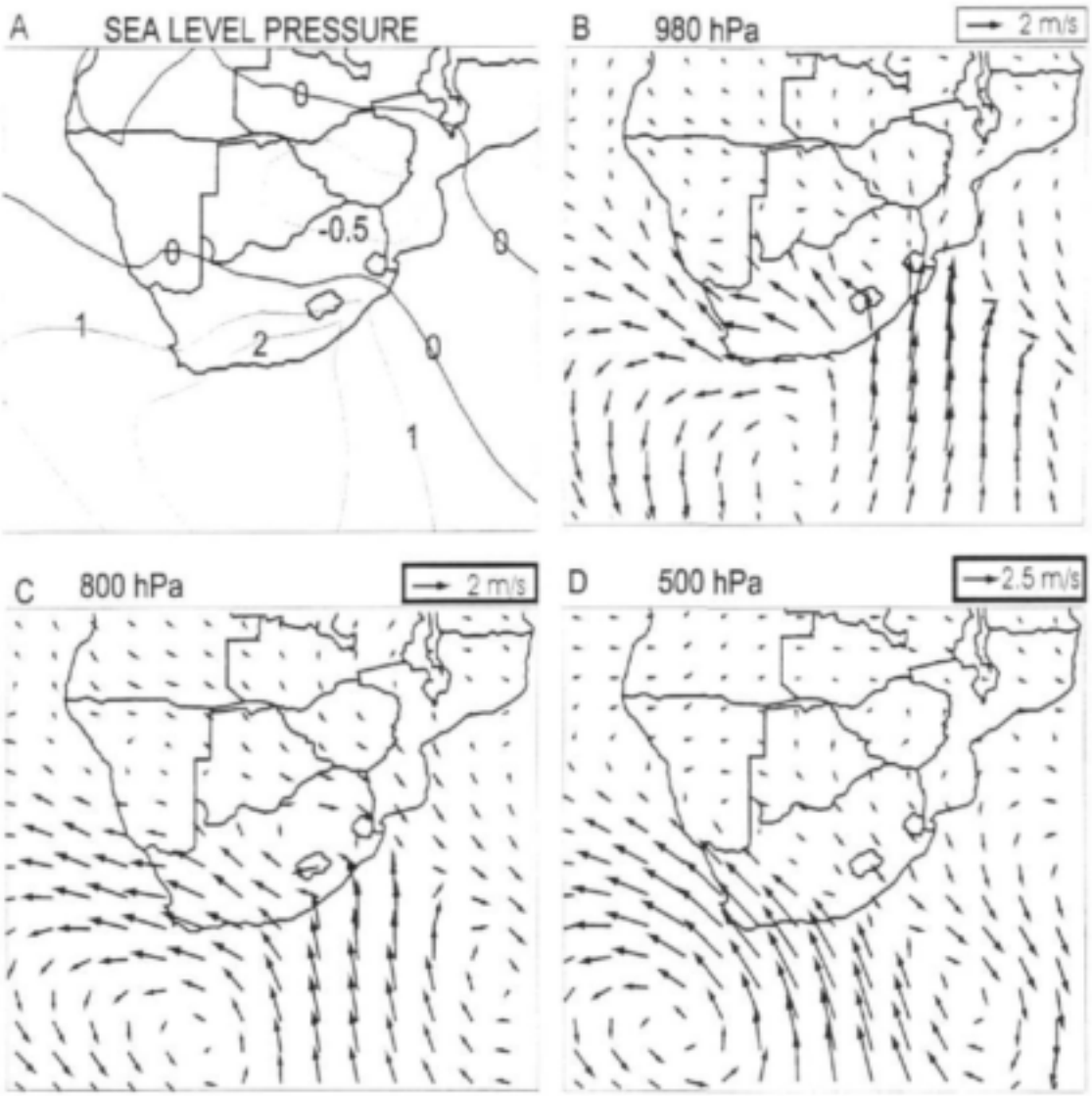

Figure 5.6. Sea-level pressure (a) and wind anomaly vectors (b-d) calculated for all days on which rainfall is above average at the model grid-point located at 28.5°S, 30.5°E. Below-normal sea-level pressures are indicated by dashed lines. Wind anomaly vectors are presented for three levels: 980 hPa (b), 800 hPa (c) and 500 hPa (d). Anomaly vector magnitudes are indicated above each panel (in m/s).

5.4.2.3. *Moisture anomalies*

Specific humidity anomalies associated with above-average rainfall along the escarpment are shown in Figure 5.7a and 5.7c. At 800 hPa (Fig. 5.7a), moisture is above average in the region of convergence on the leading edge of the ridging anticyclone (cf. Fig. 5.6a). The region of above-normal moisture extends north-westwards across central South Africa, Botswana, north-east Namibia and southern Angola. In the centre of the anticyclonic anomaly, specific humidities are below-normal (dash line). The above average moistures extend throughout the troposphere between 20° and 30°S, as well as within the tropics (Fig. 5.7c). South of 30°S, and between 10° and 20°S, specific humidities are below-average.

5.4.2.4. *Vertical velocity anomalies*

When rainfall is above-average over the escarpment region, vertical velocities are anomalously upward over the Kwazulu/Natal region, indicating uplift associated with the topographic barrier (Fig. 5.7b). The anomalous upward motion is centred near 30°S, and extends through the troposphere to a level slightly above 500 hPa (Fig. 5.7d). Vertical motion is anomalously downward to the south of 30°S, indicating the presence of the anomalous anticyclonic flow. Considering the moisture, circulation and vertical motion anomalies together, above average rainfall over the escarpment region is associated with a ridging anticyclonic flow south of the subcontinent, which advects moist air onshore and upslope. As this flow encounters the topographic barrier imposed by the escarpment, it is forced to rise, producing suitable conditions for cooling, condensation and rainfall-production.

5.5. DISCUSSION AND CONCLUSIONS

A regional climate model has been nested within the output from a global climate model to provide high-resolution, process-based simulations of present (and future) climate over the southern African region. The results presented here represent the first such experiment performed over the southern African region. Assessments of the

performance of the regional model presented earlier (Joubert *et al.*, 1998) indicate a markedly improved ability to simulate the regional climate detail, over that of the global model. As such the use of nested modelling procedures represents an important advance in climate modelling capability *within* southern Africa. Despite the general improvement, significant problems exist in the regional model simulation, specifically with the representation of daily rainfall totals and frequencies. These issues have been explored further in this report.

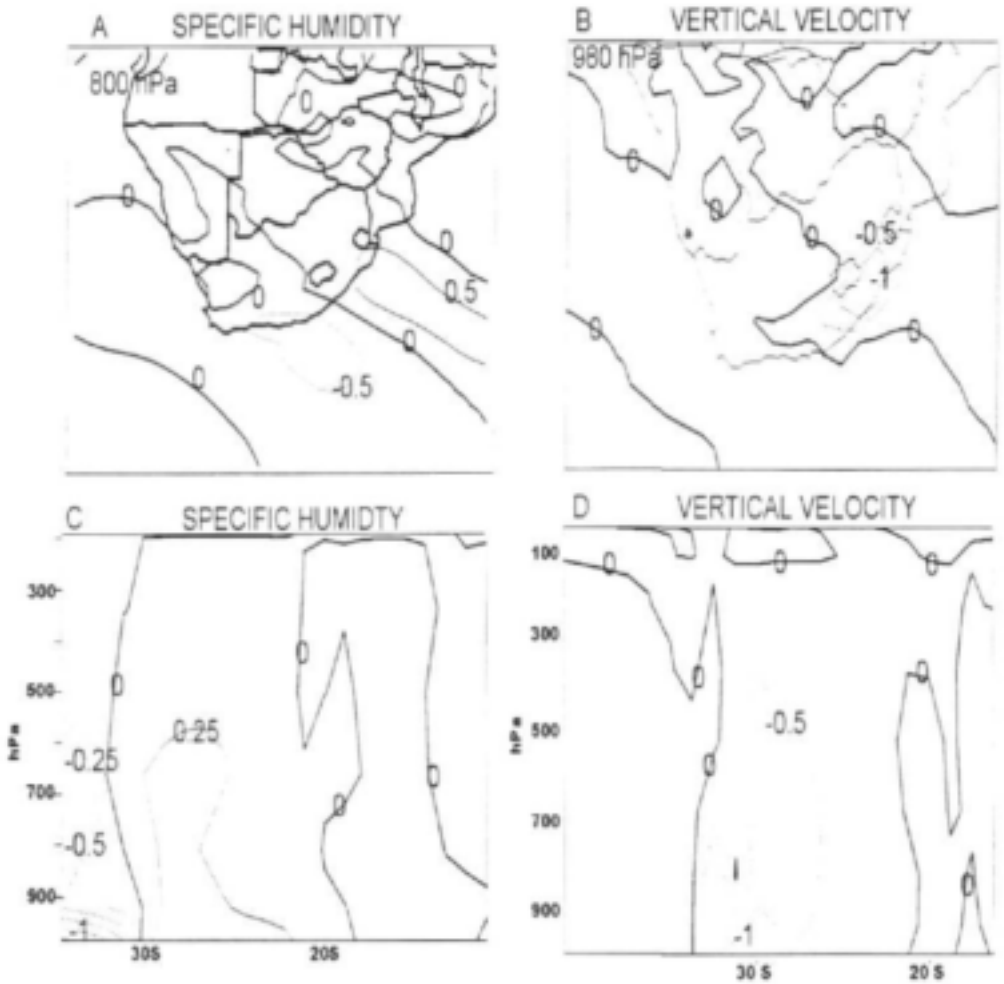

Figure 5.7. Specific humidity and vertical velocity anomalies associated with above-average rainfall over the South African escarpment. (a) 800 hPa specific humidity anomalies (in g/kg). (b) Zonal profile, through 30°E of specific humidity anomalies (g/kg). (c) Vertical velocity anomalies at 980 hPa (in Pa/s *10). (d) Zonal profile of vertical velocity anomalies, through 30°E (in Pa/s *10). Negative moisture and vertical velocity anomalies are indicated by dashed lines.

DARLAM simulates too much rain, and too many rain days over much of the eastern parts of southern Africa, and the over-estimate is most severe over regions of steep orographic gradient such as the escarpment region of South Africa. While the probability of occurrence of rainfall events of a given magnitude (expressed as the frequency of occurrence / total number of events * 100) is largely similar to observations, the fact that the model simulates up to three times the observed number of rain days in January as observed must result in an over-estimate of total rainfall.

Above average rainfall over the escarpment region is associated with anticyclone ridging to the south of the subcontinent, which extends through the troposphere to the 500 hPa level. It is worth re-iterating that observed heavy-rainfall events are often associated with a similar circulation pattern, suggesting that DARLAM reliably reproduces the circulation responses associated with above-average rainfall. Further, the circulation anomalies are localised, but occur on synoptic spatial scales, which suggests that they are likely to a response to forcing supplied by the global climate model (anomalies on this scale are unlikely to be a feature of the regional model circulation alone). The anticyclonic circulation anomaly is associated with above average moisture content, particularly in the zone of convergence on the leading edge of the ridging anticyclonic anomaly. In the immediate vicinity of the escarpment, the anomalous onshore, upslope flow results in anomalous upward motion, indicating the correct set of conditions for rainfall production.

While these results indicate sound physical reasons for rainfall to occur, they do not explain why the resulting daily rainfall statistics (both number of rain days and total daily rainfall) are so much higher than observed. One possible cause of the over-estimate relates to a known problem with the representation of flow around steep orographic barries (cf. McGregor, 1997). This relates to an over-estimate of vertical velocities in the model due to the semi-Lagrangian mountain resonance effect. In essence, the very steep orography of south-eastern southern Africa is problematic to represent in semi-Lagrangian regional model formulations. These results indicate that improvements in the simulation of regional rainfall totals will only result from further development of the regional model itself.

CHAPTER 6

SUMMARY AND CONCLUSIONS

The main objective of the Modelling Extreme Rainfall Over Southern Africa project (WRC Project Number K5/805/0/1) was to improve the existing understanding of the processes responsible for the generation of heavy rainfall over southern Africa. The goal in this project was to improve forecast skill of extreme events on a wide range of time scales. Despite the fact that the project has been foreshortened by more than a year, several important advances in our understanding of extreme rainfall events, and in the approaches available to analyse and predict them have been made:

- The CSU RAMS model has been used extensively, in conjunction with the Group's kinematic trajectory model, to improve the understanding of the moisture sources and transports associated with heavy rainfall events, such as the flood event of 11-16 February 1996. The combination of mesoscale numerical modelling and trajectory analysis has proved a useful tool in the analysis of both mesoscale atmospheric circulation and the identification of important moisture pathways. The general circulation for the period 11 to 16 February is well modelled with the RAMS regional scale numerical model and creates a three-dimensional perspective not available before. The trajectory model provides a useful depiction of parcel transport, giving an indication of possible moisture sources throughout the analysis period.

  For the duration of the 11-16 February 1996 event, the subtropical Indian Ocean to the south and east of Madagascar provided moisture for the genesis of precipitation. Of particular interest is the absence of a significant moisture supply from tropical areas to the north, or from the equatorial Indian Ocean. Presumably the development of the west coast trough and the tropical low over Madagascar diverted the tropical moisture away from the country. The

commonly held premise that atmospheric moisture is predominantly derived from the equatorial Indian Ocean during extreme rainfall events over South Africa appears to be inaccurate. Given favourable synoptic conditions, significant rainfall events can occur over South Africa with moisture supplied from the subtropical latitudes of the Indian Ocean. Research of this nature must continue in order to determine if moisture sources for rainfall over South Africa are event-specific or indeed are derived predominantly from the equatorial Indian Ocean.

- The United Kingdom Meteorological Office seasonal rainfall forecast for southern Africa for January - April 1996 suggested that conditions would be dry over much of the subcontinent north of South Africa, and close to average over South Africa itself. Flood conditions were experienced. The failure of the general circulation model to indicate wet conditions may be related to a limitation in the model's control climate: the northward progression of the westerlies during autumn occurs too early and effectively results in a premature end to the rainfall season. As a result, the model may be inherently unable to produce reliable seasonal forecasts for the second half of the season. The causes of this model-limitation deserve further investigation and may result in significant improvements in forecast skill if the problem can be resolved.

- Backward kinematic trajectory analysis of air mass transport associated with tropical cyclone Demoina (late January 1984) indicate that the primary source of moisture for the tropical cyclone was highly localised and associated with the vortex itself. Trajectories indicate an inflow from the east into the system from the central tropical Indian Ocean, associated with very rapid uplift of moisture from the surface to above 500 hPa within the walls of the cyclone itself. A secondary airflow pattern from the South Atlantic region introduces colder, drier air from the south-west, which is generally descending as it reaches the location of the cyclone vortex. It is hypothesised that this inflow provides a wedge of more stable, colder air against which the uplift in the cyclone can occur.

- The focus of climate modelling research within the Group has shifted from *global* climate model of regional climate, to the simulation of regional climate using nested *regional* models. The CSIRO limited area model (DARLAM) has been nested within the output from the CSIRO9 GCM to provide high-resolution, process-based simulations of present (and future) climate over the southern African region. In general, the regional climate models is much better-able to simulate regional climate detail than the forcing GCM, although significant problems exist in the simulation of daily rainfall totals and frequencies.

  DARLAM simulates too much rain, and too many rain days over much of the eastern parts of southern Africa, and the over-estimate is most severe over regions of steep orographic gradient such as the escarpment region of South Africa. Simulated adjustments in synoptic-scale circulation and moisture fields closely resemble observed anomalies during periods of above-average rainfall, indicating that DARLAM reliably reproduces the circulation responses associated with above-average rainfall. While these results indicate sound physical reasons for rainfall to occur, they do not explain why the resulting daily rainfall statistics (both number of rain days and total daily rainfall) are so much higher than observed. One possible cause of the over-estimate relates to a known problem with the representation of flow around steep orographic barriers. Further improvements in the representation in the regional model of processes responsible for rainfall production, particularly over regions of steep orography are required in order to improve the simulation daily rainfall over southern Africa.

An important aspect of most of the analyses presented in this report has been the source and transport of moisture associated with heavy rainfall events. The central and western portion of the *subtropical* Indian Ocean appears to be an important source of moisture for most of the extreme rainfall events discussed above. This finding is contrary to the existing knowledge, which suggests that the most important source region for moisture is the *tropical* Indian Ocean. A need exists to define clearly the sources and transport of moisture for rainfall over the southern African

region. This is possibly best achieved by defining a moisture transport climatology for the region – the subject of a forthcoming Water Research Commission-funded research project in collaboration with the Climate System Analysis Group at the University of Cape Town.

In conclusion the Climatology Research Group wishes to extend its thanks to the Water Research Commission for their support of this research during the past two years.

CHAPTER 7

PUBLICATIONS

7.1. REFEREED PUBLICATIONS

Crimp, S.J. and Mason, S.J., 1998: The extreme precipitation event of 11 to 16 February 1996 over South Africa, *Met. Atmos. Phys.*, submitted.

Joubert, A.M., Katzfey, J.J. and McGregor, J.L., 1998: Daily rainfall simulations over southern Africa using a regional climate model, *S. Afr. J. Sci.*, in preparation.

Joubert, A.M., Katzfey, J.J., McGregor, J.L. and Nguyen, K.C., 1998: Simulating mid-summer climate over southern Africa using a nested regional climate model, *J. Geophys. Res.*, accepted.

Joubert, A.M., Tennant, W. and Crimp, S.J., 1998: Air mass transport and associated mositure sources during cyclone Demoina, January 1984, *S. Afr. J. Sci.*, submitted.

Mason, S. J. 1997: Recent developments in seasonal forecasting of rainfall, *Water SA*, 23, 57-62.

7.2. CONFERENCE PRESENTATIONS

Joubert, A.M., Katzfey, J.J. and McGregor, J.L., 1998: Daily rainfall simulations over southern Africa using a regional climate model, *Conference on the Role of Topography in Modelling Regional Weather and Climate*, Abdus Salam International Centre for Theoretical Physics, Trieste, Italy, 22-26 June, 1998.

Mason, S.J., 1997: Climate predictability and potential applications of forecasts for the benefit of water resources management, *International Workshop on Weather and*

Climate-based Technologies to Benefit Water Resource Management, Pretoria, South Africa, 14-16 April 1997. (Invited opening address)

Mason, S.J., 1997: Seasonal climate forecasting, *First Regional Training Course on Practical Applications of Seasonal-to-Interannual Climate Prediction to Decision-Making in Agriculture and Water Resources Management in Africa*, Niamey, Niger, 30 June - 8 August 1997. (Invited speaker)

Mason, S.J., 1997: The status of climate forecasting in southern Africa, *Action Planning in Response to Seasonal Climate Forecasting for Mozambique*, Maputo, Mozambique, 15-16 September 1997. (Invited speaker)

Mason, S.J., Mimmack, G.M., Waylen, P.R., Rajaratnam, B. and Harrison, J.M., 1997: Changes in extreme rainfall events in South Africa, *Workshop on Indices and Indicators for Climate Extremes*, Asheville, North Carolina, U. S. A., 3-6 June 1997. (Invited speaker)

CHAPTER 8

REFERENCES

Cosjin, C. and Tyson, P.D., 1996: Stable discontinuities in the atmosphere over South Africa. *S. Afr. J. of Sci.* **92** 381-386.

Crimp, S. J., 1997: A sea-surface temperature sensitivity test using the Colorado State University Regional Atmospheric Modelling System. *S. Afr. J. Sci.*, **93**, 133-141.

D'Abreton, P. C., 1996: Lagrangian kinematic and isentropic trajectory models for aerosol and trace gas transport studies in Southern Africa. *S. Afr. J. Sci.*, **92**, 157--170.

D'Abreton, P. C., Lindesay, J. A., 1993: Water vapour transport over Southern Africa during wet and dry early and late summer months. *Int. J. Climatol.*, **13**, 151-170.

D'Abreton, P. C., Tyson, P. D., 1995: Divergent and non-divergent water vapour transport over Southern Africa during wet and dry conditions. *Meteorol. Atmos. Phys.*, **55**, 47--59.

D'Abreton, P. C., Tyson, P. D., 1996: Three-dimensional kinematic trajectory modelling of water vapour transport over Southern Africa. *WaterSA*, **22**, 297--306.

D'Abreton, P. C., Tyson, P. D., 1998: Transport and recirculation of aerosols off southern Africa: macroscale plume structure. *Atmos. Env.*, in press.

Davies, J R, Rowell, D P and Folland, C K (1997). North Atlantic and European seasonal predictability using an ensemble of multi-decadal AGCM simulations. *International Journal of Meteorology*, in press.

Dorman, J.L., and P.J. Sellers, 1989: A global climatology of albedo, roughness length and stomatal resistance for atmospheric general circulation models as represented by the simple biosphere model (SiB), *J. Appl. Meteorol., 28*, 833-855.

Edwards, M., 1997: Heavy rain and floods in South Africa during January February 1996: Synoptic review. *Proceedings of the Fifth International Conference on Southern Hemisphere Meteorology and Oceanography*. Boston: American Meteorological Society, 9--10.

Eliassen, A., 1975: Decay and transformation rates for SO_2, as estimated from emission data, trajectories and measured air concentrations. *Atmos. Environ.* **9** 425-229.

Eliassen, A., 1978: The OECD study of long-range transport of air pollutants: Long-range transport modelling. *Atmos. Environ.* **17** 479-487.

Eliassen, A., 1980: A review of long-range transport modelling. *J. Appl. Meteorol.* **19** 231-240.

Garstang, M., Tyson, P.D., Swap, R., Edwards, M., Källberg, P. and Lindesay, J.A., 1996: Horizontal and vertical transport of air over Southern Africa. *J. Geophys. Res. SAFARI Special Issue* **101**.

Gillooly, J.F. and Dyer, T.G.J., 1979: Spatial Variations in Rainfall during abnormally wet and dry years. *S. Afri. J. of Sci.* **75** 261-262.

Giorgi, F., 1990: Simulation of regional climate using a limited area model nested in a general circulation model, *J. Clim., 3*, 941-963.

Giorgi, F., 1995: Perspectives for regional earth system modeling, *Global and Planetary Change, 10*, 23-42.

Giorgi, F., and L.O. Mearns, 1991: Approaches to the simulation of regional climate change: A review, *Rev. Geophys., 29*, 191-216.

Giorgi, F., and M.R. Marinucci, 1991: Validation of a regional atmospheric model over Europe: Sensitivity of wintertime and summertime simulations to selected physics parameterisations and lower boundary conditions. *Quart. J. Roy. Meteorol. Soc., 117*, 1171-1206.

Giorgi, F., and M.R. Marinucci, 1996: Improvements in the simulation of surface climatology over the European region with a nested modeling system, *Geophys. Res. Lett., 23*, 273-276.

Giorgi, F., C.S. Brodeur, and G.T. Bates, 1994: Regional climate change scenarios over the United States produced with a nested regional climate model, *J. Clim., 7*, 375-399.

Giorgi, F., G.T. Bates, and S.J. Nieman, 1993a: The multiyear surface climatology of a regional atmospheric model over the western United States, *J. Clim., 6*, 75-95.

Giorgi, F., M.R. Marinucci, and G.T. Bates, 1993b: Development of a second-generation regional climate model (RegCM2). Part I: Boundary-layer and radiative transfer processes, *Mon. Wea. Rev., 121*, 2794-2813.

Harrison, M. S. J., 1986: *A Synoptic Climatology of South African rainfall variations.* Unpublished PhD Thesis, University of the Witwatersrand, 341 pp.

Harrison, M. S. J., 1988: Rainfall and precipitable water relationships over the central interior of South Africa, *S. Afr. Geog. J.*, **70**, 100--111.

Hudson, D.A., 1997: Southern African climate change simulated by the GENESIS GCM, *S. Afri. J. Sci., 93*, 389-403.

James, I. N., Anderson, D. L. T., 1984: The seasonal mean flow and distribution of large scale weather systems in the Southern Hemisphere: the effects of moisture transports. *Quarterly Journal of the Royal Meteorological Society*,

110, 943--966.

Joubert, A M (1997). Simulations by the Atmospheric Model Intercomparison Project of atmospheric circulation over southern Africa. *International Journal of Climatology*, **17**, 1129 - 1154.

Joubert, A.M., 1994: Simulations of southern African climatic change by early generation general circulation models, *WaterSA*, *20*, 315-322.

Joubert, A.M., 1995: Simulations of southern African climate by early generation general circulation models, *S. Afr. J. Sci.*, *91*, 85-91.

Joubert, A.M., 1997: Simulations by the Atmospheric Model Intercomparison Project of atmospheric circulation over southern African, *Int. J. Climatol.*, *17*, 1129-1154.

Joubert, A.M., and B.C. Hewitson, 1997: Simulating present and future climates of southern Africa using general circulation models, *Prog. Phys. Geog.*, *21*, 51-78.

Joubert, A.M., and P.D. Tyson, 1996: Equilibrium and fully-coupled GCM simulations of future southern African climates, *S. Afr. J. Sci.*, *92*, 471-484.

Joubert, A.M., Katzfey, J.J., McGregor, J.L. and Nguyen, K.C., 1998: Simulating mid-summer climate over southern Africa using a nested regional climate model, *J. Geophys. Res.*, accepted.

Kalnay, E., and others, 1996: The NCEP/NCAR 40-year Reanalysis Project, *Bull. Amer. Meteorol. Soc.*, *77*, 437-472.

Kalnay, E., Kanamitsu, M., Kistler, R., Collins, W., Deaven, D., Gandin, L., Iredell, M., Saha, S., White, G., Woollen, J., Zhu, Y., Chelliah, M., Ebisuzaki, W., Higgins, W., Janowiak, J., Mo, KC., Ropelewski, C., Wang, J., Leetma, A., Reynolds, R., Jenne, R. and Dennis, J., 1996: The NCEP/NCAR 40-year reanalysis project. *Bull. Amer. Meteorol. Soc.* 77 437-471.

Kowalczyk, E. A., J. R. Garratt, and P. B. Krummel, 1994: Implementation of a soil-canopy scheme into the CSIRO GCM - regional aspects of the model response, *Tech. Pap. 32*, 59 pp., Commonwealth Sci. and Ind. Res. Org., Melbourne.

Krishnamurti, T.N., Fuelberg, H.E., Sinha, M.C., Oosterhof, D., Bensman, E.L. and Kumar, V.B., 1993: The meteorological environment of the tropospheric ozone maximum over the tropical South Atlantic Ocean. *J. Geophys. Res.* **98** 10621-10641.

Kroese, N. J., Mittermaier, M. P., Terblanche, D. E., 1997: The flood event during February 1996 in the Vaal river catchment: A Radar rainfall and streamflow study. *Proceedings of the Fifth International Conference on Southern Hemisphere Meteorology and Oceanography*. Boston: American Meteorological Society, 13--14.

Lindesay, J.A. and Jury, M.R., 1991: Atmospheric circulation controls and characteristics of a flood event in central South Africa. *Int. J. of Climatol.* **11** 609-627.

Mahrer, Y., Pielke, R. A., 1977: Parameterization of the atmospheric surface layer. *J. Atmos. Sci.*, **34**, 331--334.

Marinucci, M.R. and F. Giorgi, 1992: A 2 x CO2 climate change scenario over Europe generated using a limited are model nested in a general circulation model 1. Present-day seasonal climate simulation, *J. Geophys. Res.*, *97*, 9989-10009.

Marinucci, M.R., F. Giorgi, M. Beniston, M. Wild, P. Tschuck, A. Ohmura, and A. Bernasconi, 1995: High resolution simulations of January and July climate over the western Alpine region with a nested regional climate modeling system, *Theor. Appl. Climatol.*, *51*, 119-138.

Mason, S J, Joubert, A M, Cosijn, C and Crimp, S J (1996). Review of the current state of seasonal forecasting techniques with applicability to southern Africa. *WaterSA*, **22**, 203 - 209.

Mason, S. J., Jury, M. R., 1997: Climatic variability and change over southern Africa: a reflection on underlying processes. *Prog. Phys. Geog.*, **21**, 23--50.

McGee, 0. S., 1971: The meridional flux of atmospheric water vapour across 30°S over South Africa. *S. Afr. Geog. J.*, **53**, 78--83.

McGee, 0. S., 1972: The content of water vapour in the atmosphere over southern Africa. *S. Afr. Geog. J.*, **4**, 25--32.

McGee, 0. S., 1975: The transport of water vapour in the atmosphere over southern Africa. *S. Afr. Geog. J.*, **57**, 135--147.

McGee, 0. S., 1978: A note on the inter-annual consistency of atmospheric water vapour content over South Africa. *S. Afr. Geog. J.*, **6**, 31--34.

McGee, 0. S., 1986: The distribution of water vapour in the atmosphere over South Africa. *S. Afr. Geog. J.*, **68**, 117--131.

McGregor, J.L., 1987: Accuracy and initialization of a two-time-level split semi-Lagrangian model, Short and Medium-Range Numerical Weather Prediction, T. Matsuno, Ed., Special Volume of the *J. Meteor. Soc. Japan*, 233-246.

McGregor, J.L., 1997: Regional climate modelling, *Meteorol. Atmos. Phys.*, *63*, 105-117.

McGregor, J.L., and K. Walsh, 1993: Nested simulations of perpetual January climate over the Australian region, *J. Geophys. Res.*, *98*, 23283-23290.

McGregor, J.L., and K. Walsh, K., 1994: Climate change simulations of Tasmanian precipitation using multiple nesting, *J. Geophys. Res.*, *99*, 20889-20905.

McGregor, J.L., H.B. Gordon, I.G. Watterson, M.R. Dix, and L.D. Rotstayn, 1993: The CSIRO 9-Level Atmospheric General Circulation Model, *Tech. Pap. 26*, 89 pp., Commonwealth Sci. and Ind. Res. Org., Melbourne.

Nassor, A. and Jury, M.R., 1997: Intra-seasonal climate variability of Madagascar. Part 2: Evolution of flood events. *Meteorol. Atmos. Phys.* **64** 243-254.

Poolman, E. and Terblanche, D., 1984: Tropiese siklone Demoina en Imboa. *SA Weather Bureau News Letter.* **420** 37-43.

Renwick, J.A., J.J. Katzfey, K.C. Nguyen, and J.L. McGregor, 1998: Regional model simulations of New Zealand climate. *J. Geophys. Res., 103*, 5973-5982.

Sun, L., H.M. Semazzi, and F. Giorgi, 1997: Toward the development of a seasonal climate prediction system for eastern Africa, *Eighth Symposium on Global Change Studies*, pp. 254-259, American Meteorological Society, Boston, Mass.

Taljaard, J. J., 1958: *South African Air-Masses: Their Properties, Movement and Associated Weather.* Unpublished PhD Thesis, University of the Witwatersrand, 221 pp.

Taljaard, J. J., 1986: Change of rainfall distribution and circulation patterns over southern Africa in summer. *Int. J. Climatol.*, **6**, 579--592.

Taljaard, J. J., 1987. The anomalous climate and weather systems over South Africa during summer 1975-1976. *S. Afr. Weath. Bur. Tech. Pap.*, **16**, 80 pp.

Taljaard, J. J., 1990: The cloud bands of South Africa. *S. Afr. Weath. Bur. Tech. Pap.*, **493**, 6--8.

Tremback, C. J., Tripoli, G. J., Cotton, W. R., 1985: A regional atmospheric modelling system. In Zannetti, P. (ed.), *Proceedings of the International Conference on the Development and Application of Computer Techniques to Environmental Studies*. Boston: Computational Mechanics Publications, 601--607.

Triegaardt, D.O. and Kits, A., 1963: Die drukveld by verskillende vlakke oor suidelikke Afrika en aangrensende oseane tydens reën en droë periodes in

suid-Transvaal en noord-Vrystaat gedurende die 1960-61 somer. *SA Weather Bureau News Letter* **168** 37-43.

Triegaardt, D.O., van Heerden, J. and Steyn, P.C.L., 1991: Anomalous precipitation and floods during February 1988. *SA Weather Bureau Technical Paper* **23** 53pp.

Tripoli, G. J., Cotton, W. R., 1982: The Colorado State University three-dimensional cloud/mesoscale model - 1982. Part I: General theoretical framework and sensitivity experiments. *J. Atmosphériques*, **16**, 185--219.

Tyson, P. D., 1986: *Climatic Change and Variability in Southern Africa*. Cape Town: Oxford University Press, 220 pp.

Tyson, P. D., 1997: Atmospheric transport of aerosols and trace gases over southern Africa. *Prog. Phys. Geog.*, **21**, 179--101.

Tyson, P.D., Garstang, M. and Swap, R., 1996: Large-scale recirculation of air over Southern Africa. *J. of Appl. Meteorol.* **35** (11).

Tyson, P.D., Garstang, M., Swap, R., Källberg, P. and Edwards, M., 1996: An air transport climatology for subtropical Southern Africa. *Int. J. of Climatol.* **16** 265-291.

van den Heever, S.C., 1995: Modelling tropical-temperate troughs over Southern Africa. Unpublished M.Sc. Dissertation, University of the Witwatersrand. 216pp.

Walsh, K. and J.L. McGregor, 1997: An assessment of simulations of climate variability over Australia with a limited area model, *Int. J. Climatol.*, *17*, 201-233.

Walsh, K., and J.L. McGregor, 1995: January and July climate simulations over the Australian region using a limited-area model, *J. Clim.*, *8*, 2387-2403.

Walsh, K., and J.L. McGregor, 1996: Simulations of Antarctic climate using a limited area model, *J. Geophys. Res.*, *101*, 19093-19108.

Watterson, I.G., M.R. Dix, H.B. Gordon, and J.L. McGregor, 1995: The CSIRO nine-level atmospheric general circulation model and its equilibrium present and doubled CO_2 climates, *Aust. Meteorol. Mag.*, *44*, 111-125.